UPTEC X 07 050
Examensarbete 20 p
September 2007

Analysis of oncogenic mutations in a panel of colon carcinoma cell lines

Sara Kiflemariam

UPPSALA UNIVERSITET

Molecular Biotechnology Programme

Uppsala University School of Engineering

UPTEC X 07 050	**Date of issue 2007-09**

Author

Sara Kiflemariam

Title (English)

Analysis of oncogenic mutations in a panel of colon carcinoma cell lines

Title (Swedish)

Abstract

Colon carcinoma is developed in colon epithelial cells by accumulation of sequential genetic alterations in oncogenes and tumour suppressor genes, controlling cell growth and differentiation. In this study a series of colon carcinoma cell lines, derived at the Ludwig Institute for Cancer Research in Melbourne, Australia, have been analysed for mutations, predominantly in the Wnt signalling and ERK-MAPK pathways, being relevant for the initiation and progression of colon cancers.

Keywords

Colon carcinoma, oncogenes, tumour suppressor genes, mutations, APC, microsatellite instability, ERK-MAPK pathway, Wnt signalling pathway

Supervisors

Dr. Francesca Walker

Ludwig Institute for Cancer Research, Melbourne, Australia

Scientific reviewer

Carina Hellberg

Ludwig Institute for Cancer Research, Uppsala, Sweden

Project name	Sponsors
Language **English**	Security
ISSN 1401-2138	Classification
Supplementary bibliographical information	Pages **53**

Biology Education Centre Biomedical Center Husargatan 3 Uppsala

Box 592 S-75124 Uppsala Tel +46 (0)18 4710000 Fax +46 (0)18 555217

Analysis of oncogenic mutations in a panel of colon carcinoma cell lines

Sara Kiflemariam

Populärvetenskaplig sammanfattning

Cancer är en av de vanligaste dödsorsakerna i världen, där tarm-och ändtarmscancer har blivit identifierad som den fjärde största orsaken till cancer-relaterade dödsfall. Cancern utvecklas och fortskrider i tarmepitelceller genom att ackumulera avvikelser, såsom mutationer, i gener som normalt förhindrar att en cell omvandlas till en tumörcell. Exempel på gener med stort inflytande i utvecklingen av tarm-och ändtarmscancer är Adenomatosis Polyposis Coli (APC), K-Ras och B-Raf. Mutationer i APC, som är mutaterad i ungefär 80% av alla tarm- och ändtarmscancrar, tros vara ett förstadium i utvecklingen av cancern men mutationer i andra gener är nödvändiga för fortskridningen och invasionen av annan vävnad i kroppen.

Syftet med projektet har varit att analysera nio tarm-och ändtarmscancercellinjer, framtagna vid Luwig Institute for Cancer Research i Melbourne, Australien, för mutationer i olika gener, till exempel APC, K-Ras och B-Raf. Resultaten visade att flera cellinjer uppvisade mutationer i mer än en gen och att mutationer i både K-Ras och B-Ras aldrig påträffades i en och samma cellinje.

Mutationsanalyser på gener i tumörceller har försett forskare med en fundamental inblick i utvecklingen och fortskridningen av tarm-och ändtarmscancer. Celler med mutationer i flera gener utgör en ideal modell för att utvärdera varje gens betydelse i utvecklingen av cancern, men även för att undersöka genens normala roll i cellulära processer, såsom celltillväxt och celldifferentiering.

Examensarbete 30 hp i Molekylär bioteknikprogrammet

Uppsala universitet september 2007

Table of contents

Abbreviations

Abs	Absorbance
APC	Adenomatous Polyposis Coli
CIN	Chromosomal Instability
DDW	Double Distilled Water
EDTA	Ethylenediaminetetraacetic acid
EtBr	Ethidium Bromide
FCS	Foetal Calf Serum
HNPCC	Hereditary Non-Polyposis Colon Cancer
HEPES	N-2-HydroxyEthylPiperazine-N'-2-Ethane Sulfonic acid
HT-PBS	Human Tonicity-Phosphate Buffered Saline
LIM	Ludwig Institute Melbourne
LRP	Low-density lipoprotein-receptor Related Protein
MMR	Mismatch Repair
MSI	Microsatellite Instability
MSS	Microsatellite Stability
Mut	Mutant
MW	Molecular Weight
PCR	Polymerase Chain Reaction
qRT-PCR	Quantitative Real-Time PCR
RPMI	Roswell Park Memorial Institute
Wt	Wild type

1. Introduction

Cancer is a leading cause of death worldwide and colorectal cancer has been identified as the fourth largest cause of cancer-related deaths (http://www.who.int/cancer/en). Through accumulation of sequential genetic alteration in oncogenes and tumour suppressor genes controlling cell growth and differentiation, the cancer initiates in the epithelial cells of the colon from hyperproliferative foci, progressing to adenomatous polyps and eventually to carcinomas [1,2]. Oncogenes, such as K-Ras, become activated by a single "gain-of-function" mutation, which result in proteins with an abnormal expression of the normal gene product. The activation of oncogenes stimulates cell growth and inhibits apoptosis as well as differentiation. Tumour suppressor genes, such as Adenomatous Polyposis Coli (APC), are on the contrary affected by "loss-of-function" mutations. Non mutated tumour suppressor genes contribute to the inhibition of cell growth, stimulation of differentiation and apoptosis [3]. In order for a tumour suppressor gene to fully lose its function both alleles have to be inactivated. This can occur through loss of heterozygosity (LOH) where a cell loses part of the chromosome carrying the wild type allele [4].

The development of colon cancers is thought to pass through three stages before becoming an invasive carcinoma. The first stage is a small benign adenoma or polyp, which commonly occurs in healthy individuals without developing into cancer. During the second stage the adenoma grows and becomes more malignant enabling progression of some adenomas to carcinomas. Finally the adenomas progress to invasive carcinomas [5].

It is believed that mutations in the APC gene are an initiating event in the development of colorectal cancer. Additional mutations in APC mutated cells, such as in K-Ras and the tumour suppressor gene p53, will lead to growth and to the progression from adenomas to carcinomas [6] (Figure 1). In order to create an environment that is permissive for alterations in tumour suppressor genes and oncogenes, genomic instability has to take place early on in the tumourigenesis [7]. According to several studies APC mutations occur in colorectal cancer with a high frequency, approximately 80%, and the result of these mutations is the constitutive activation of the Wnt signalling pathway [6].

Colorectal cancer can be classified into three different categories depending on the cancer risk and the hereditary influence. The first category is sporadic cancers which constitutes about 60% of the cases and display no family history and no germline mutation that accelerates the cancer development. Secondly familial cancers, approximately 30%, have at least one family member with colon cancer but there are no detectable germline mutations. The last category is hereditary colon cancers, about 10% of the cases, where germline mutations in target genes have been inherited, such as in Hereditary Non-Polyposis Colon Cancer (HNPCC) where germline mutations occur in the DNA mismatch repair (MMR) genes [8] and in Familial Adenomatosis Coli (FAP), where APC is mutated [9].

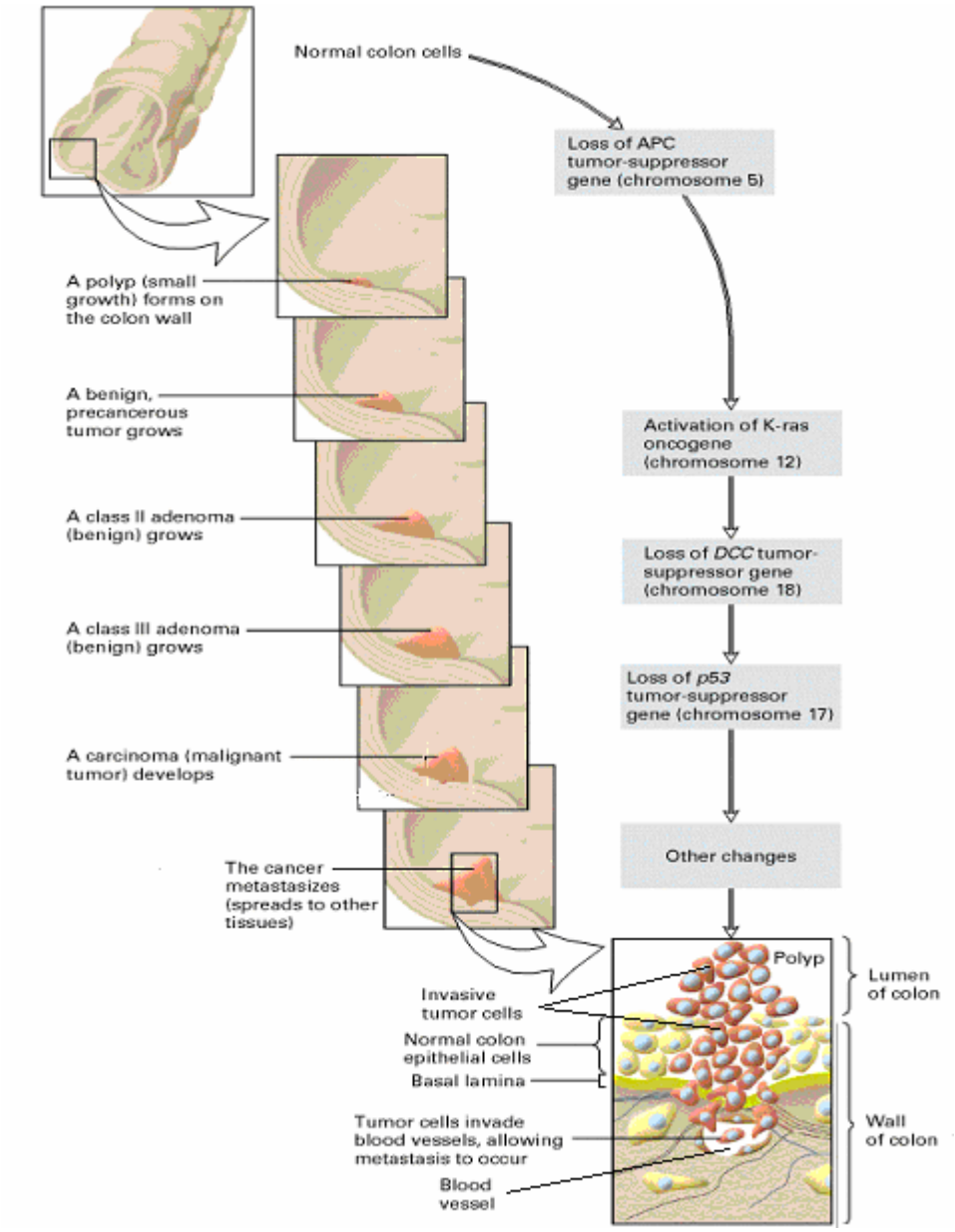

Figure 1. A schematic view of the development and metastasis of colorectal cancer and the associated genetic changes. A mutation in APC in a single epithelial cell causes the cell to divide and form a polyp, a mass of localized benign tumour cells. Additional mutations within these cells generate malignant cells that continue to divide and invade the surrounding tissue, including blood vessels. Adapted from Vogelstein B. and Kinzler K., *Trends in Genetics*,1993 9:101.

2. Aim of the project

The project can be divided into two separate parts. The main goal has been to characterize nine colorectal carcinoma cell lines (LIM 1215, LIM 1863, LIM 1899, LIM 2099, LIM 2408, LIM 2463, LIM 2537, LIM 2550 and LIM 2551), derived at the Ludwig Institute for Cancer Research, Melbourne, for mutations in pathways relevant to colon cancer such as the ERK-MAPK pathway and the Wnt signalling pathway. This information will then aid in the assessment of the contribution of each pathway to the tumour phenotype, which can be studied by selectively blocking each pathway using RNA interference, small molecule inhibitors or neutralizing antibodies.

A second part of the project has been to analyze the nine LIM cell lines for mutations in microsatellites, with particular reference to two genes (TGFβRII and BAX) involved in cell growth and survival. Knowledge of the mutations introduced by changes at the microsatellite level will allow the generation of antibodies to frame-shift induced peptides, which can be used as diagnostic or analytical tools in identifying mutated peptides in different tumour samples.

3. Background

3.1 The ERK-MAPK pathway

The Extracellular Signal-Related Kinase Mitogen-Activated Protein Kinase (ERK-MAPK) pathway is one of three major subfamilies of the MAPK pathway and is crucial for cell proliferation and differentiation. This pathway has shown to be hyperactivated in approximately 30% of all human cancers. Also, several studies have demonstrated that the activation and overexpression of proteins in this pathway play a central role in the progression of colorectal cancer. The key components of this signalling pathway are a series of serine-threonine kinases, through which the signals controlling growth and differentiation can be transmitted from growth factor receptors on the cell surface to the nucleus.

When a ligand, such as a cytokine or a growth factor, binds to its transmembrane receptor, for example the Epidermal Growth Factor (EGF), the receptor becomes activated through the phosphorylation of specific tyrosine residues on its intracellular domain. This leads to the recruitment of adaptor proteins such as the growth factor receptor bound protein 2 (Grb2) which associates with the guanine nucleotide exchange factor son of sevenless (SOS) to activate members of the Ras family (H-Ras, N-Ras and K-Ras) (Figure 3)[10].

The Ras protein alternates between its active guanosine trihosphate (GTP) bound form and its inactive guanosine diphosphate (GDP) bound form. The protein contains a GTP/GDP-binding domain and a GTPase domain, which binds GTPase activating protein

(GAP); through this domain it hydrolyzes GTP to GDP thereby returning to the inactive state (Figure 2). Conversely, the conformation of Ras changes upon binding to SOS enabling the dissociation of Ras from GDP and allowing the binding of GTP instead resulting in sustained activation [11].

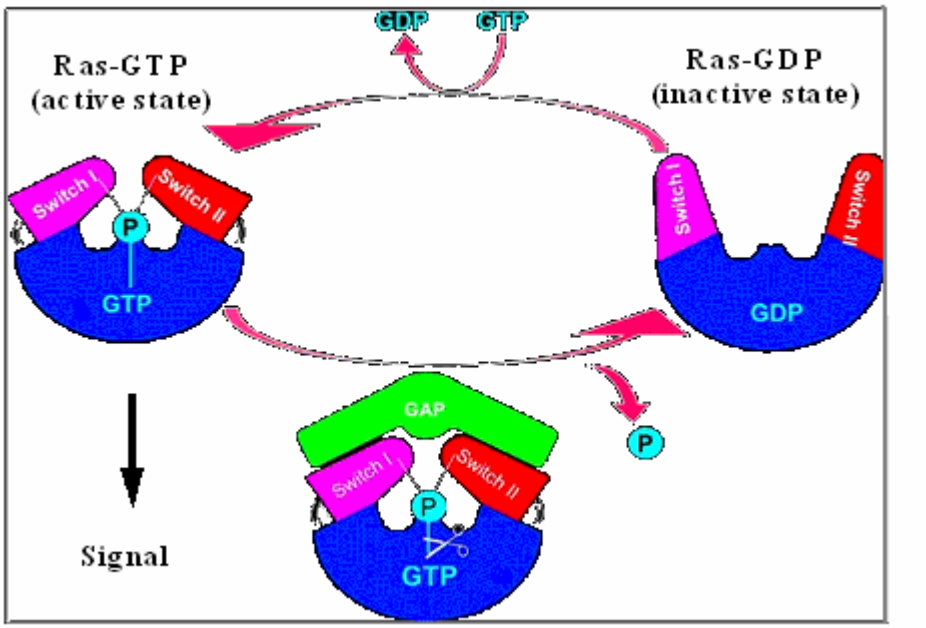

Figure 2. Schematic view of Ras in its active (GTP-bound) and inactive (GDP-bound) forms. Binding of GAP to active Ras stimulates the GTPase activity of Ras and hydrolyzes GTP to GDP returning Ras to its inactive state. Adapted from Kratz CP., Niemeyer CM., Zenker M., *Journal of Molecular Medicine*, 2007 Mar;85(3):223-31.

Ras activation enables the recruitment of the Raf protein, another key regulator of the ERK-MAPK pathway, to the plasma membrane where it is in turn activated through phosphorylation at serine and threonine residues [10]. Raf is a serine-threonine kinase which through transferring phosphate groups to other proteins alters their function [12]. To date there are three known Raf genes; A-Raf, B-Raf and c-Raf. Upon activation, Raf phosphorylates serine residues in the kinases MEK1 and MEK2, leading to the phosphorylation of members of the ERK family and their subsequent translocation to the nucleus. This result in the phosphorylation and activation of diverse transcription factors allowing the transcription of genes involved in cell proliferation and differentiation (Figure 3).

Mutations at specific sites in either Ras or Raf lead to constitutive activation, bypassing the need for extracellular-signal mediated activation and mimicking the positive regulation of cell proliferation by growth factors and cytokines [10].

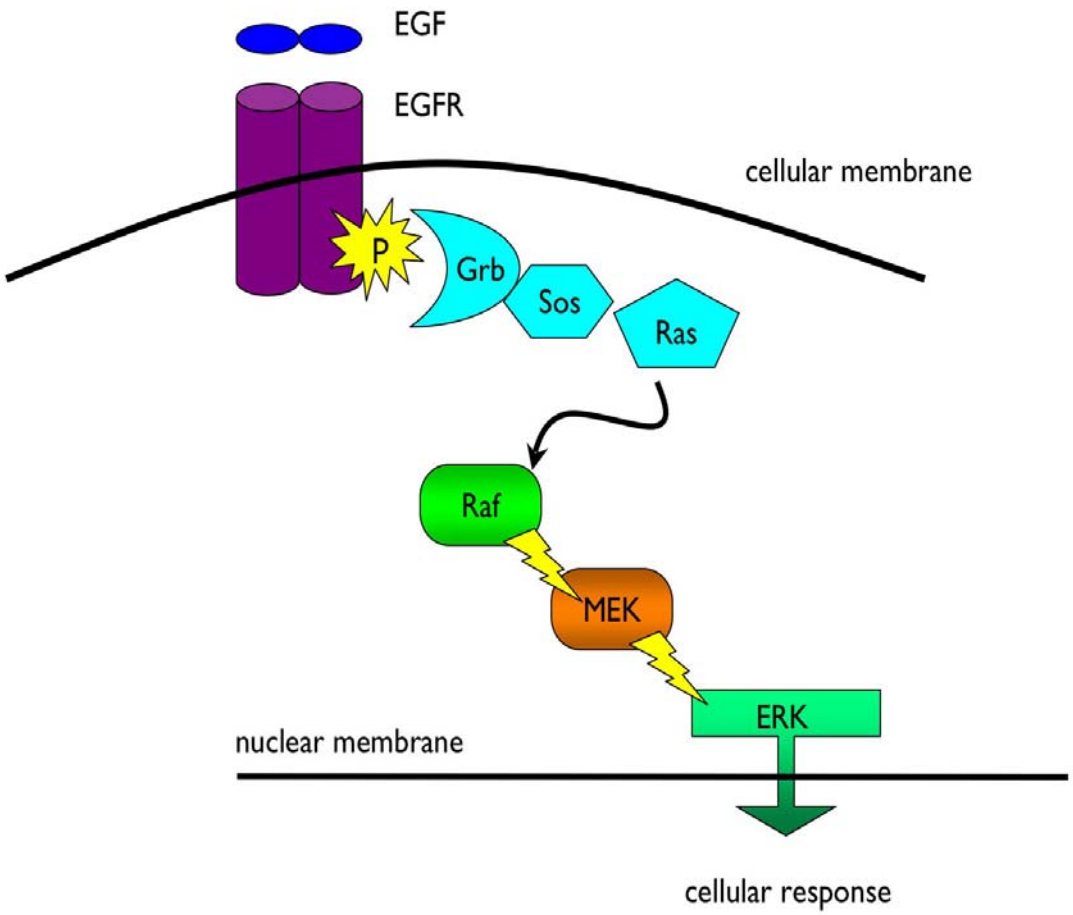

Figure 3. Overview of the ERK-MAPK pathway. When a receptor is bound to its ligand it becomes activated through phosphorylation leading to the recruitment of a number of proteins, such as Grb and SOS. This results in the activation of Ras which in turn recruits and activates Raf leading to phosphorylation of MEK and ERK kinases resulting in their subsequent translocation to the nucleus where transcription is initiated. Reproduced with permission from the PhD thesis of Nicholas Simon Aberle (University of Melbourne, 2007).

3.2 K-Ras and B-Raf in colon cancer

3.2.1 K-Ras

Mutations in the oncogene K-Ras are present in approximately 50% of colorectal cancers [13] occurring at about the same frequency in both familial and sporadic colorectal cancers [14] . The mutations are thought to be a relatively early event in the progression of colon cancers. Previous studies have demonstrated that K-Ras mutations show a higher frequency in MSS colon cancers than in MSI [15].

The common mutations in the Ras protein result in constitutive activation regardless of whether or not there is an external stimulus. The activating point mutations

have primarily been found in codons 12 (GGT) and 13 (GGC) [16], but they also occur in codons 19 (TTG) [13] and 61 (CAA) [16]. It has been demonstrated that codons 12 and 13 harbour approximately 90% of all K-Ras mutations in colon cancer [15]. Codons 12 and 13 form part of the GTP/GDP exchange domain [13] while codon 61 is found in the GTPase domain [14]. Consequently, the Ras protein mutated at these codons remains in the active GTP-bound form and continuously activate the ERK-MAPK pathway [11].

It has been demonstrated that mutations in codon 12 are predominant in environmentally associated cancers, such as lung, bladder and colon cancer associated with tobacco smoking. In sporadic colorectal cancers mutations in codon 12 are predominant whereas in HNPCC mutations in codon 13 are more common. A reason for this might be that sporadic colorectal cancers are more susceptible to damage in certain DNA sequences by environmental factors while inheritance is the key factor for HNPCC cancers. Substitution of guanine (G) to adenine (A) at the second position in codon 12 resulting in an amino acid change from glycine to aspartic acid is the most frequent alteration in both MSI and MSS colorectal cancers. The most common K-Ras mutation in HNPCC occurring in 55% of cases is a G to A substitution at the second position in codon 13 also resulting in a glycine to aspartic acid amino acid change. The G to A mutation has turned out to be difficult to restore even without MMR deficiency. This might be related to the purine structure of G and A, consisting of a pyrimidine ring fused together with an imidazole ring [14].

Prior studies have shown that mutations in K-Ras and B-Raf are mutually exclusive, i.e. cells from the same tumour sample displaying a K-Ras mutation will most likely not display a B-Raf mutation and vice versa [16]. Mutual exclusion strongly supports the notion that Ras and Raf are part of the same pathway.

3.2.2 B-Raf

The oncogene B-Raf is mutated in 10-15% of sporadic colorectal cancers [10]. Studies show that B-Raf mutations are more frequent in MSI sporadic colorectal cancer, where the MSI has arisen from hypermethylation of the *hMLH1* promoter [15]. The most common activating mutation in B-Raf, accounting for approximately 90% of all B-Raf mutations in human cancers [17], occurs at codon 600, where a thymine (T) has been substituted for an A resulting in an amino acid change from the neutral valine (V) to the negatively charged amino acid glutamic acid (E). This leads to the constitutive activation of Raf, most likely by mimicking the transient phosphorylation of threonine at position 599 and serine at position 602, which occur during normal signalling [12]. The V600E mutation is the only B-Raf mutation that has been shown to upregulate the ERK-MAPK pathway without being accompanied by K-Ras mutations [15]. Other less common B-Raf mutations have been shown to require the interaction with Ras to become phosphorylated and activated [18].

3.3 The Wnt signalling pathway

The Wnt signalling pathway has a significant role in cell growth, differentiation and apoptosis during normal embryonic development of different tissues [6]. Several studies have demonstrated a strong link between the inappropriate, continuous activation of the Wnt signalling pathway and cancer [3].

The Wnt factors are secreted proteins which through binding to their transmembrane receptors Frizzled and co-receptors LRP activate a signalling cascade inside the cell. When the Wnt factors bind to their receptors a cytoplasmic protein called Dishevelled is recruited to the membrane where it becomes activated. Active Dishevelled then recruits the scaffolding protein Axin, a key regulator in the β-catenin destruction complex which consists of Axin, β-catenin, APC, casein kinase 1 (CK1) and glycogen synthase kinase 3 (GSK3). Recruitment of Axin to the membrane leads to failure in assembling the β-catenin destruction complex enabling the accumulation of β-catenin in the cytoplasm and its subsequent translocation to the nucleus. β-catenin can then bind transcription activators such as T-Cell Factor (TCF) and Lymphoid Enhancer Factor (LEF) and initiate transcription of target genes involved in tumour invasion and progression, such as the cell cycle regulators cyclin D1 and c-myc (Figure 4B) [6]. The TCF/LEFs posses DNA binding domains but are deficient in transcriptional activity and repress transcription in the absence of β-catenin by interacting with co-repressors, such as Groucho. β-catenin on the other hand contains transactivation domains but lacks DNA binding activity. It is therefore only through binding to each other that transcription of target genes can be initiated [19].

In the absence of the Wnt factors, Dishevelled is not activated and the β-catenin destruction complex can form leading to the phosphorylation of β-catenin at specific serine and threonine residues at the N-terminus by CK1 and GSK3 [6]. CK1 phosphorylates β-catenin at serine residue 45 which enables the subsequent phosphorylation at serine residues 33 and 37 and at threonine residue 41 by GSK3 [20]. These phosphorylations steps all take place at the scaffolding protein Axin, which arranges the kinases and β-catenin in a correct position [19]. Phosphorylated β-catenin is targeted for degradation in proteasomes by the ubiquitin E3 ligase β-TrCP (Figure 4A) [6]. Single mutations in any of the four phosphorylation sites in β-catenin lead to its stabilization indicating the importance of these sites for efficient degradation of the β-catenin protein [20].

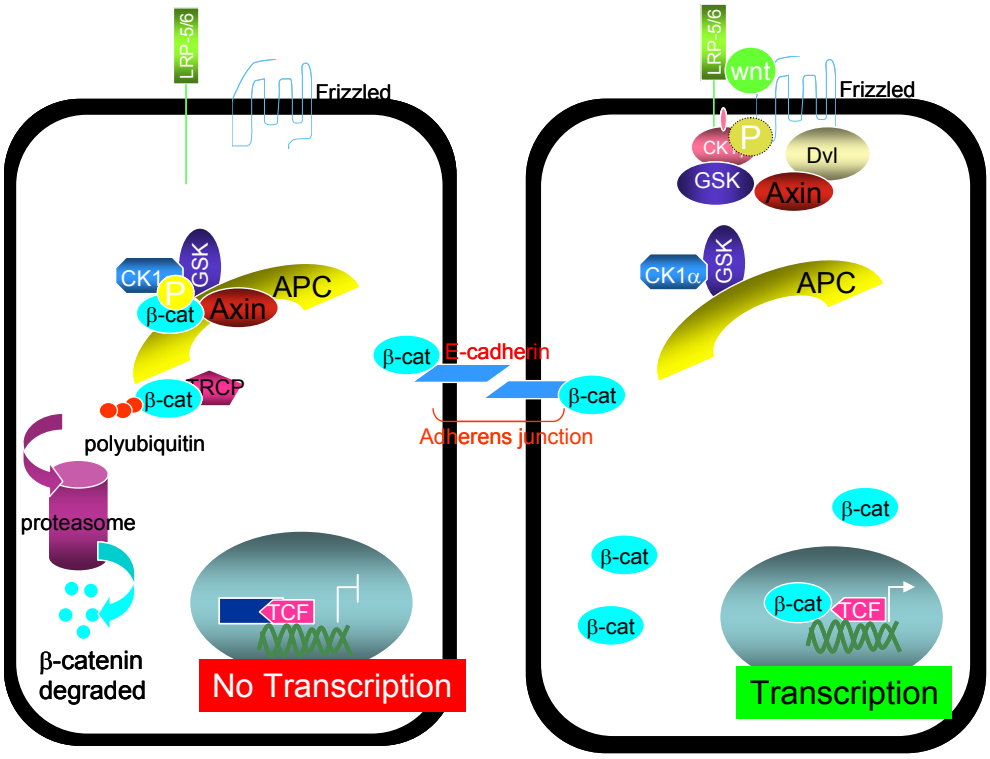

Figure 4. Schematic view of the Wnt signalling pathway. **A)** In the absence of Wnt factors. Inactive Dishevelled results in the formation of the β-catenin destruction complex leading to the phosphorylation and degradation of β-catenin. **B)** In the presence of Wnt factors. Active Dishevelled recruits Axin which leads to failure in assembling the β-catenin destruction complex enabling the accumulation of β-catenin in the cytoplasm and its subsequent translocation to the nucleus where transcription of target genes can take place. β-cat, β-catenin; Dvl, Dishevelled.

Axin-APC interaction promotes the phosphorylation of APC by GSK3 and leads to an increase in β-catenin degradation when compared with the unphosphorylated form of APC [21]. It has been reported that expression of certain target genes can lead to negative feedback loops, which block the activity of the Wnt signalling pathway, for example β-TrCP is activated by Wnt signalling [19].

β-catenin also plays a role in cell-cell adhesion by binding to cadherin cell adhesion molecules, for example E-cadherin in epithelial cells, which links E-cadherin to the actin cytoskeleton [19]. These cell-cell junctions are essential for the formation and preservation of epithelial layers [4].

When components of the β-catenin destruction complex, for example APC, β-catenin or Axin, are mutated the assembly of the destruction complex is obstructed leading to the constitutive activation of the Wnt signalling pathway, possibly independent of Wnt factors. Previous studies have shown that because colorectal cancer cells frequently express Wnt factors, the Wnt signalling pathway can be suppressed by Secreted Frizzled Related Proteins (SFRPs), which interfere with the binding of Wnt factors to their receptors. Because of this the SFRP genes in colorectal cancer cells are often inactivated through hypermethylation [6].

3.4 APC in colon cancer

The tumour suppressor gene APC plays a crucial role in several cellular processes, such as in cell cycle regulation, cell migration, cell adhesion, cytoskeletal reorganization and chromosomal stability [6]. The gene contains 16 exons encoding a 312 kDa protein comprised of 2843 amino acids. The last exon is the largest, containing more than 75% of the coding region of the gene. This region also harbours most of the mutations found in APC. Three 15 amino acid repeats and seven 20 amino acid repeats, all β-catenin binding sites, are located in the central region of the APC protein (blue and orange in Figure 5). Furthermore, three SAMP (serine, alanine, methionine and proline) repeats for axin-binding are interspersed between the seven 20 amino acid repeats (pink in Figure 5) [22].

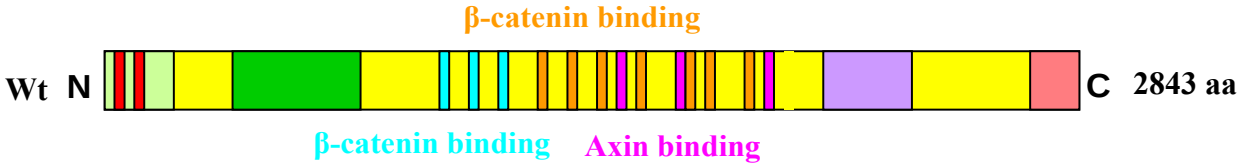

Figure 5. The APC protein and the binding sites for β-catenin and Axin. N, N-terminus; C, C-terminus; aa, amino acid.

Studies have demonstrated that only the 20 amino acid repeats and not the 15 amino acid repeats are essential for the downregulation of β-catenin. Therefore truncated APC proteins often retain all 15 amino acid repeats and only one or two of the 20 amino acid repeats [23]. It has been shown that excessive accumulation of β-catenin in the nucleus lead to apoptosis, thus making it essential for mutant APC to retain some β-catenin binding sites in order to allow for adequate accumulation of nuclear β-catenin and the subsequent activation of target genes [4].

APC has been shown to be mutated in approximately 80% of colorectal cancers [6]. About 60% of these mutations occur in a mutation cluster region which is situated in the middle of the coding sequence [3], from codon 1286 to codon 1585 [22]. APC mutation leads to frame-shift and a premature stop resulting in a truncated form of the protein where significant amounts of the C-terminal and binding sites for Axin and β-catenin are lost. Consequently the assembly of the β-catenin destruction complex fails resulting in the stabilization and the subsequent translocation of β-catenin to the nucleus where transcription is initiated (Figure 6).

It has been reported that expression silencing of APC through hypermethylation is another, although rare, way of inactivating the gene [23]. Because APC possesses a suppressor function both alleles at the APC locus have to be inactivated for tumour progression to take place. Studies have demonstrated that the introduction of wild type APC in colorectal cancers containing only mutant APC proteins resulted in lower levels of β-catenin [24].

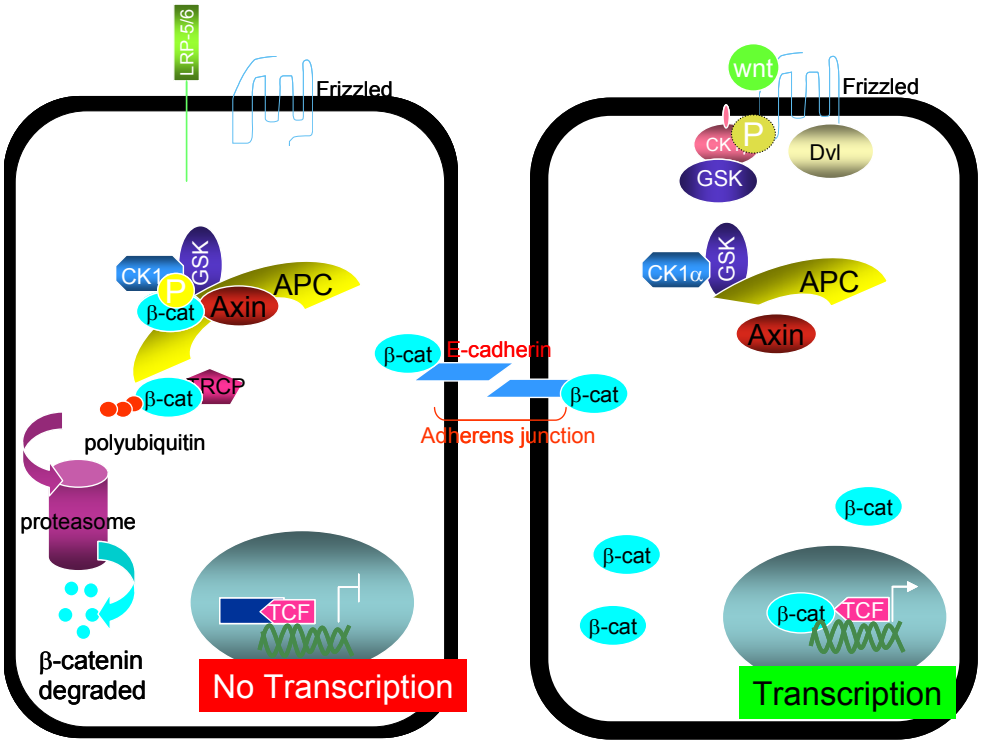

Figure 6. Schematic view of the Wnt signalling pathway. **A)** In the absence of Wnt factors. Inactive Dishevelled results in the formation of the β-catenin destruction complex leading to the phosphorylation and degradation of β-catenin. **B)** APC mutation mimics the Wnt-mediated activation of the pathway. The β-catenin destruction complex cannot be assembled, which enables the accumulation of β-catenin in the cytoplasm and its subsequent translocation to the nucleus where transcription of target genes can take place. β-cat, β-catenin; Dvl, Dishevelled.

3.5 Microsatellite instability

Microsatellites are short coding or non-coding sequence repeats, such as $[A]_n$, found throughout the entire human genome. During DNA replication the DNA polymerase and the template strand in a microsatellite can occasionally dissociate and re-anneal incorrectly, resulting in an inaccurate number of microsatellite repeat units in the template and in the newly synthesized strand. These errors together with the base-base mismatches caused by the DNA polymerase and which escaped its proof-reading activity are corrected by the DNA MMR system. The MMR system degrades the wrongly synthesized section providing the DNA polymerase a second chance in generating an accurate copy of the template strand [25].

Microsatellite instability (MSI) is a type of genetic instability where the MMR system has been inactivated, occurring in approximately 15% of sporadic colon cancers [8] and in 90% of HNPCC [26]. This can arise through mutations in the MMR genes; *hMLH1*, *hPMS1*, *hPMS2, hMSH2*, *hMSH3* and *hMSH6* [8], especially in *hMLH1* and *hMSH2* which account for approximately 90% of all known MMR gene mutations [14], or through hypermethylation of the *hMLH1* promoter leading to loss of the hMLH1 protein, which

occurs more commonly, in about 70% of sporadic MSI colon cancers. The defective MMR proteins can be detected either at the genetic level through DNA sequencing, or at the protein level through immunohistochemistry [8].

MSI promotes tumourigenesis by generating mutations in target genes that contain microsatellites in their coding regions, most frequently in the tumour suppressor genes transforming growth factor β receptor type II (TGFβRII) and BAX [27]. TGFβRII mediates epithelial cell growth inhibition and has been found to be mutated in approximately 90% of MSI colon cancers[28] while BAX, a promoter of apoptosis, is mutated in about 50%[29]. The mutations results in insertions or deletions at the repetitive regions leading to frame-shifts; these in turn result in functionally inactive proteins and cause the generation of a new immunogenic peptide sequence at the carboxy terminus. Although the peptides generated by mutations in TGFβRII and BAX are synthesized in most MSI cancer cells they are not present in all cancer cells. It is therefore of interest when considering a potential cancer vaccine derived from these peptides, that multiple epitopes are combined. It is believed that an immunized individual will be able to recognize and react to these mutated peptides generated by frame-shift mutations [26]. Studies have shown that people with MSI colon cancers have a higher survival rate than people with microsatellite stable (MSS) cancers, but the reason for this remains unclear [30]. One hypothesis is that frame-shift induced peptides present in MSI colon cancers are capable of eliciting cytotoxic immune responses against tumour cells [28].

The majority of colon cancers are aneuploid and MSS, displaying genetic instability at the chromosomal level, known as chromosomal instability (CIN), whereas MSI colon cancers are diploid and show instability at the nucleotide level [31].

Tumours with MMR deficiency are typically different to MMR proficient tumours, which have mutations in APC and K-Ras, in regards to age, gender, differentiation and localization of tumour. MSI tumours are predominantly found in the proximal colon of elderly women and they are often less differentiated [32]. However, according to Shimizu *et al.* dysfunction of the Wnt signalling pathway occurs frequently both in MSI and MSS colorectal cancers [21].

3.6 TGFβRII and BAX in colon cancer

3.6.1 TGFβRII

The TGFβRII gene contains a repetitive sequence of ten adenine (A) and mutations within this microsatellite region are found in 90% of MSI colon cancers. TGFβRII binds the transforming growth factor β (TGFβ), an epithelial growth inhibitor, when it is in a complex with the type I receptor. When this gene, or the TGFβRI gene, is inactivated in cancer cells through mutations the responsiveness to the growth inhibitor is lost. Mutations in the microsatellite region lead to frame-shifts and result in truncated TGFβRII proteins with novel peptides at the carboxy terminus. Because these peptides are recognized by the human body as foreign, they are potential cancer vaccine candidates [28].

3.6.2 BAX

The BAX protein promotes apoptosis upon activation by the related protein Bcl-2, an inhibitor of apoptosis. The BAX gene contains a microsatellite repeat of eight guanine (G) and is mutated in approximately 50% of MSI colon cancers. BAX mutated cells might display a reduced capability to activate apoptosis when receiving a death signal thus conferring a survival advantage to the tumour cells[29].

4. Materials and Methods

4.1 Cell lines

The cell lines used in this project were derived from human primary colon carcinomas, and all cell lines except for HT-29 were established at the Ludwig Institute for Cancer Research, Melbourne Branch, abbreviated by LIM [33-37]. The following LIM cell lines were analyzed; LIM 1215, LIM 1863, LIM 1899, LIM 2099, LIM 2408, LIM 2463, LIM 2537, LIM 2550, LIM 2551.

Table 1. Overview of the origin and characteristics of the LIM cell lines. Microsatellite status was determined by immunohistochemistry (Dr. David Williams, Dept. of Pathology, Royal Melbourne Hospital, Victoria, Australia).

Cell line	Origin	Morphology	Microsatellite status
LIM 1215	Colon carcinoma HNPCC	Loosely adherent	MSI
LIM 1863	Sporadic colon carcinoma	Organoids, gland structure	MSS
LIM 1899	Sporadic colon carcinoma	Adherent	MSS
LIM 2099	Liver metastasis from colon carcinoma	Adherent, spindly moderate pleomorphism	MSS
LIM 2408	Colon carcinoma	Adherent, mild nuclear pleomorphism	MSI
LIM 2463	Tubulovillus adenoma of the rectum	Organoids, gland structure, secrete mucus	MSS
LIM 2537	Colon carcinoma	Loosely adherent, organoids	MSI
LIM 2550	Colon carcinoma	Loosely adherent	MSI
LIM 2551	Colon carcinoma HNPCC	Loosely adherent	MSI

4.2 Cell culture

All cells were cultured at 37 ºC in 10% CO_2 on 100 mm plates in RPMI-1640 (Gibco, 31800089) supplemented with 0.1 M 10-2 Thioglycerol, 25 U/L Insulin, 1 mg/L Hydrocortisone and 10% FCS.

4.3 Harvesting of cells

Due to the different morphology of the cells, adherent or organoids, the harvesting process varies.
Adherent cells: The medium was removed with no risk of losing any cells. 2 ml Trypsin (0.1% Trypsin and 0.02% Versene) was added to the each plate in order to detach the cells from the plastic. Because the optimal operating temperature for Trypsin is 37 ºC the cells were incubated at this temperature for 5-10 min, or until the cells were not adherent anymore when examined under a microscope. 5 ml HT-PBS was added to each plate and the cell suspensions were transferred to centrifuge tubes and spun at 1500 rpm for 5 min. The supernatant was discarded.
Organoid cells: Cells were re-suspended in their culture medium by vigorous pipetting. The medium+cells was collected, transferred to centrifuge tubes and spun at 1500 rpm for 5 min, followed by the removal of the supernatant.

4.4 Isolation of genomic DNA from cultured cells

Genomic DNA from each cell line was isolated using the DNeasy® Tissue Kit (150) (Qiagen, Hilden, Germany and Germantown, United States). Each cell pellet, both adherent and organoid, was resuspended in 200 µl HT-PBS and then transferred to Eppendorf tubes. 20 µl proteinase K and 200 µl Buffer AL were added to each sample, vortexed and incubated at 70 ºC for 10 min. Proteinase K, a serine protease, ensures clean and high quality genomic DNA by inactivating RNases and DNases. Then, 200 µl of 100% ethanol were added to each sample and mixed thoroughly by vortexing. Each of the samples was transferred into a DNeasy Mini Spin Column placed in a 2 ml collection tube, all included in the kit. The samples were centrifuged at 8000xg for 1 min and the collection tubes with the flow-through were discarded. The DNeasy Mini Spin Column was placed in a new collection tube and 500 µl Buffer AW1 was added. The samples were centrifuged at 8000xg for 1 min followed by the removal of the collection tubes with the flow-through. Once again the DNeasy Mini Spin Column was placed in a collection tube and 500 µl Buffer AW2 was added, followed by centrifugation at 13 000 rpm for 3 min. The collection tubes with the flow-through were discarded. It is of high importance that the membrane of the DNeasy Mini Spin Column dries completely since carryover of ethanol may interfere with subsequent elution. The DNeasy Mini Spin Columns were placed in 2 ml Eppendorf tubes and 200 µl Buffer AE was added. The

samples were incubated at room temperature for 1 min and then centrifuged at 8000xg for 1 min to elute the DNA.

The DNA concentration of each sample was measured at an absorbance of 260 nm using a UV-Visible spectrophotometer. Each sample was diluted 100x in Tris Buffer (10 mM, pH 8). The DNA concentration of the PCR products was calculated using the following formula:

$$DNAconc(ng/\mu l) = Abs_{260} * 50 * 100,$$

where 100 is the dilution factor and 50 is the multiplication factor. For the subsequent PCR reactions the DNA samples were diluted in DDW to make stocks of 25 ng/µl.

4.5 Primer design

The software program Primer 3 was used for designing primers to be utilized in PCR, qRT-PCR and for sequencing. The DNA sequence of interest was copied and pasted in a field and specific conditions for the primers were selected. The product size of the DNA was chosen to be between 200-500 base pairs, while the primer size was between 18-26 base pairs where 20 was the optimal size. The annealing temperature (T_m) was chosen to range from 59-63 ºC, the optimal T_m being 60 ºC. The primer contents of GC for each primer should lie between 40% and 60%, where 50 % is optimal. The software program then picks the primers that best fulfill these criteria. The primers, purchased from Sigma Genosys (Sydney, Australia), were supplied at an original concentration of 100 µM, and each primer was diluted to 10 µM in DDW before use.

Table 2. Primer sequences and product sizes for B-Raf. F, forward primer; R, reverse primer.

Gene	Primer sequence	Product size
B-Raf exon 11	F: 5'-TCCCTCTCAGGCATAAGGTAA-3'	224
	R: 5'-CGAACAGTGAATATTTCCTTTGAT-3'	
B-Raf exon 15	F: 5'-TCATAATGCTTGCTCTGATAGGA-3'	313
	R: 5'-GGCCAAAAATTTAATCAGTGGA-3'	

Table 3. Primer sequences and product sizes for K-Ras. F, forward primer; R, reverse primer.

Gene	Primer sequence	Product size
K-Ras exon 2	F: 5'-GTGTGACATGTTCTAATATAGTCA-3'	214
	R: 5'-GAATGGTCCTGCACCAGTAA-3'	
K-Ras exon 3	F: 5'-GGTGCTTAGTGGCCATTTGT-3'	292
	R: 5'-AAAGAAAGCCCTCCCCAGT-3'	

Table 4. Primer sequences and product sizes for APC. F, forward primer; R, reverse primer.

Gene	Primer sequence	Product size
APC exon 16 AA	F: 5'-CAGGCAAATCCTAAGAGAGAACA-3'	556
	R: 5'-TGATGAAGAGGAGCTGGGTAA-3'	
APC exon 16 BB	F: 5'-GCTCAAGCTTGCCATCTCTT-3'	552
	R: 5'-TATGGGCAGCAGAGCTTCTT-3'	
APC exon 16 CC	F: 5'-TTTGCAGATCTCCACCACTG-3'	504
	R: 5'-TGTGAAGGACTTTGCCTTCC-3'	
APC exon 16 A	F: 5'-AAGAAGCTCTGCTGCCCATA-3'	527
	R: 5'-CACATTCCTGCTGTCCAAAA-3'	
APC exon 16 B	F: 5'-GGAAGGCAAAGTCCTTCACA-3'	579
	R: 5'-GAGCTGATTCTGCCTCTTGG-3'	
APC exon 16 C	F: 5'-GAGGCAGAATCAGCTCCATC-3'	562
	R: 5'-CATTCCACTGCATGGTTCAC-3'	
APC exon 16 D	F: 5'-CCCTAGAACCAAATCCAGCA-3'	536
	R: 5'-CACTCAGGCTGGATGAACAA-3'	
APC exon 16 E	F: 5'-GGCATTATAAGCCCCAGTGA-3'	596
	R: 5'-ACAGGCAGCTGACTTGGTTT-3'	
APC exon 16 F	F: 5'-ATGCCAACAAAGTCATCACG-3'	545
	R: 5'-TGATTTTTGTTGGGTGCAGA-3'	
APC exon 16 G	F: 5'-CCCAAAGGGAAAAGTCACAA-3'	524
	R: 5'-GCTGATTGTTGGTTGGAGGT-3'	
APC exon 16 H	F: 5'-ACCTCCAACCAACAATCAGC-3'	663
	R: 5'-AGCAGCAGCAGCTTGATGTA-3'	
APC exon 16 I	F: 5'-GCTGCTGCTGCATGTTTATC-3'	582
	R: 5'-AGGTCTTGAAGGGGTCGAAT-3'	
APC exon 16 J	F: 5'-ATTCGACCCCTTCAAGACCT-3'	528
	R: 5'-GAGTTTGTGCCTGGGACCTA-3'	
APC exon 16 K	F: 5'-TAGGTCCCAGGCACAAACTC-3'	527
	R: 5'-CAGCAGGTGCCATTTGATAA-3'	
APC exon 16 L	F: 5'-CCAAGTATCCGCAAAAGGAA-3'	536
	R: 5'-GAGTCACTCTGGCAGCAACA-3'	
APC exon 16 M	F: 5'-TGGAACGTACCCCATTCAGT-3'	542
	R: 5'-GAAGTTGGGATGGGATGCTA-3'	

Table 5. Primer sequences and product sizes for TGFβRII. F, forward primer; R, reverse primer.

Gene	Primer sequence	Product size
TGFβR2 microsatellite	F: 5'-CCTCGCTTCCAATGAATCTC-3'	421
	R: 5'-TGCCCCAGTCAACCATATTT-3'	
TGFβR2 STOP	F: 5'-CATGAACCCACTTCCTGACA-3'	345
	R: 5'-CAGCAGCTCTGTGTTGTGGT-3'	

Table 6. Primer sequences and product sizes for BAX. F, forward primer; R, reverse primer.

Gene	Primer sequence	Product size
BAX	F: 5'-GAGTGACACCCCGTTCTGAT-3'	283
	R: 5'-TTAGGGGAGGAGGAGAATGC-3'	

Table 7. Primer sequences and product size for APC in qRT-PCR. F, forward primer; R, reverse primer.

Gene	Primer sequence	Product size
APC exon 9 and 10	F: 5'-CACCTCGAAGGCTGACAAGT-3'	105
	R: 5'-GCAAAGTTCGCGACATATCAT-3'	

4.6 Polymerase Chain Reaction (PCR)

To amplify the specific DNA fragments PCR was used. All of the following components: 10xPCR Buffer, 25 mM $MgCl_2$ and Taq polymerase, were provided by the Ludwig Institute for Cancer Research in Melbourne, and the ΔdNTP was purchased from Amersham Pharmacia Biotech, Inc (now known as GE Healthcare Life sciences). Prior to running a normal PCR reaction (Table 8) the conditions for each primer, such as annealing temperature, had to be optimized. Therefore, a test PCR (Table 9) was first run for each primerset.

Table 8. Normal PCR scheme.

PCR components	x1 (µl)
10xBuffer	5
$MgCl_2$ [25 mM]	4
dNTP [2 µM]	5
Forward primer [10 µM]	2
Reverse primer [10 µM]	2
Taq polymerase [5U/µl]	2
DNA [25 ng/µl]	4
DDW	26
Total volume	50

Table 9. Test PCR scheme.

PCR components	x1 (µl)
10xBuffer	2
$MgCl_2$ [25 mM]	1.6
dNTP [2 µM]	2
Forward primer [10 µM]	1
Reverse primer [10 µM]	1
Taq polymerase [5U/µl]	1
DNA [25 ng/µl]	2
DDW	9.4
Total volume	20

The PCR thermal cycling conditions used were:

95 °C 2 min
[95 °C 1 min Tm $_{opt}$ 1 min 72 °C 1 min] x 35 cycles
72 °C 5 min
4 °C short-term storage

Tm $_{opt}$ indicates the optimal annealing temperature for the primer. The PCR products were stored short-term at 4 °C until further processing.

4.7 Agarose gel electrophoresis

To asses the PCR products agarose gel electrophoresis was employed. A 1.5 % agarose gel solution was prepared by dissolving 1.2 g agarose in 80 ml 1xTAE buffer and 2 µl EtBr (10 mg/ml, Amresco) was added to the solution to aid in the visualization of the DNA bands under UV light. 5µl of 6x-concentrated Loading dye (0.25% Orange G and 30% Glycerol) was added to each PCR product before loading the gel. 15 µl of 1Kb+ DNA ladder (0.1 µg/ml, Gibco) was loaded in the first lane and the PCR products in the subsequent lanes. The gels were run in 1xTAE at 100 V for 30-45 min and photos were taken of the gels using a UV camera. After the electrophoresis the DNA bands were illuminated with UV by placing the gel on a light box. In the presence of DNA the EtBr fluoresces in orange, which facilitates the excision of specific bands. The bands were cut out from the gel, transferred to pre-labeled tubes and stored at 4 °C until further processed.

4.8 Purification of PCR products

In order to extract the DNA QIAEX II Agarose Gel Extraction Kit (150) (Qiagen) was used. Once the DNA bands had been excised 1 ml Buffer QX1 was added to each sample.

The QIAEXII solution was re-suspended by vortexing before adding 5 µl of it to every tube. In order to solubilize the agarose and bind the DNA the samples were incubated at 50 °C for 10 min and vortexed every 2 min to keep QIAEXII in suspension. The samples were then centrifuged at 13 000 rpm for 1 min and the supernatant was discarded. 500 µl Buffer QX1 was used to wash the pellet followed by centrifugation at 13 000 rpm for 1 min. The supernatant was discarded. This step ensures that all traces of residual agarose are removed. The samples were then washed with 500 µl Buffer PE, centrifuged using the same conditions and the supernatant was discarded. A second wash step using 1000 µl Buffer PE was performed followed by centrifugation at 13 000 rpm for 1 min and discarding the supernatant. These washing steps with Buffer PE aid in the removal of residual salt contaminants. Afterwards, the pellets were air-dried for approximately 10-15 min but without overdrying, as this could result in decreased elution efficiency. 20 µl pH 8 H_2O was added to elute the DNA and the samples were incubated at room temperature for 5 min. Elution efficiency is highly dependent on pH and because the maximum elution efficiency is attained between pH 7.0-8.5, the pH for H_2O has to be within this range. After incubation, the sample was centrifuged at 13 000 rpm for 1 min and the supernatant, now containing the purified DNA, was transferred to a pre-labeled tube.

The concentration of each DNA sample was measured using the same method as previously described but this time the DNA was diluted 20x instead of 100x in Tris Buffer (10 mM, pH 8). Therefore, the concentration of the PCR products was calculated as follows:

$$DNAconc(ng/\mu l) = Abs_{260} * 50 * 20$$

4.9 Sequencing

The DNA sequencing was done off site by the Welcome Trust Sequencing Centre at Monash University in Melbourne, Australia. Each reaction tube contained the DNA, one primer (either forward or reverse) and DDW up to a total volume of 16 µl. Depending on the product size the amount of DNA in the reaction tube differed; for products between 200-500 base pairs 10-25 ng DNA was employed and for products between 500-1000 base pairs 25-50 ng DNA was used. The amount of primer added to the reaction tube was constant at 3.2 pmol.

4.10 Analysis

The software programs used for the analysis of the sequencing results were: Editseq, Seqman (both from DNASTAR, version 5.8) and Chromas (Technelysium, version 2.23). Editseq is used for entering and manipulating DNA or protein sequences, for example when viewing the complementary sequence or translating a DNA sequence. Seqman enables the assembly and alignment of multiple sequences facilitating the analysis

process significantly. The software Chromas displays the chromatogram for each sample which provides an additional tool for analyzing the results.

4.11 Western blot

Western blot analysis was conducted in order to detect the APC protein in all the nine cell lines. This was used to confirm the results achieved by sequencing at the genomic DNA levels, and to confirm whether the APC protein in the different cell lines was full length (wt) or truncated (mut).

4.11.1 Cell harvest

1-2 days prior to performing the Western blot the cells were plated at 2-3x10^6 cells per cell line in tissue culture Petri dishes. The harvesting procedure was different for the adherent and the organoid cells.

Adherent cells: The medium was removed and the flask was rinsed once with HT-PBS, which was discarded afterward. The plates were placed on ice and 300-500 µl of ice-cold solubilization buffer was added to each plate. The cells were collected by scraping and transferred to Eppendorf tubes which were placed on ice.

Organoid cells: The medium+cells were collected into centrifuge tubes and spun at 1500 rpm for 5 min followed by the removal of the supernatant. The pellets were resuspended in 1.5 ml HT-PBS, transferred to Eppendorf tubes and collected by spinning at 13 000 rpm for 12 seconds only. The cells were resuspended in 300-500 µl of ice-cold solubilization buffer and the Eppendorf tubes were placed on ice.

All cells: Using a 1 ml syringe with a 26-gage needle the cells were disrupted by passing through the needle 5-6 times avoiding froth. The cells were incubated on ice for 15 min and then centrifuged at 13 000 rpm, 4 ºC for 30 min to pellet the insoluble material.

The supernatants, which contained the soluble cytosolic and membrane proteins, were transferred to fresh tubes. An equal amount of 4xconcentrated SDS sample buffer+β-mercaptoethanol was added to each tube and the samples were then boiled at 95 ºC for 10-15 min.

4.11.2 SDS-PAGE electrophoresis

NuPage® Novex 4-12% gels with 10 wells each 1.5 mm wide (Invitrogen) were placed in a gel tank which was filled up by NuPage MOPS buffer (Invitrogen). The first well was loaded with 20 µl of MW marker, SeeBlue® or SeeBlue® Plus (Invitrogen), followed by 30 µl of each sample in the subsequent wells. Electrophoresis was performed at 120 V for approximately two hours until the 200 kDa marker had run well into the gel, about 1.5 cm from the bottom of the well.

4.11.3 Electrophoretic transfer

For the transfer of the proteins from the gel to a membrane, 2 litres of 1:20 dilution of the stock Transfer buffer solution (Invitrogen) containing methanol to 20% final concentration were prepared. A PVDF (polyvinylidene difluoride) membrane was used, which was soaked in methanol briefly before placing it in a container with a small volume of Transfer buffer. The remaining Transfer buffer was poured into a transfer tank. In order to cool down the buffer the tank was set up in a cold room (4 ºC) over a magnetic stirrer. A gel/membrane sandwich was assembled by placing a sponge on the black side of a cassette followed by two sheets of Whatman 3MM paper (Whatman, Brentford, UK) and the gel on top of that. The membrane was then placed on the gel followed by two sheets of Whatman 3 MM paper, a sponge and the white side of a cassette. The gel/membrane sandwich was placed in the transfer tank with the black side of the transfer cassette facing the black side on the transfer tank. Transfer of the proteins from the gel to the PVDF membrane was performed at 90V overnight or at 120V for three hours at 4 ºC.

4.11.4 Immunodetection

The membrane was removed from the gel/membrane sandwich, making sure that the MW markers had been transferred. To block the non-specific binding sites the membrane was placed in HT-PBS containing 5% Skim milk powder and rocked gently for three hours at room temperature or overnight at 4 ºC. The blocking solution was removed and replaced by the primary Rabbit anti-APC antibody (H-290, 0.2 mg/ml, Santa Cruz Biotechnology, Santa Cruz, United States) diluted 1:1000 in HT-PBS with 5% Skim milk powder. The membrane was incubated with gentle agitation for three hours at room temperature or overnight at 4 ºC. The antibody solution was removed and the membrane was washed 3x10 min in TTBS. A 1:10 000 dilution in TTBS of the secondary antibody (Odyssey anti-Rabbit anti-APC antibody, 680 or 800 labelled) was prepared and the membrane was placed into it. After incubation with gentle agitation for one hour in the dark (covered in aluminum) the antibody solution was discarded and the membrane was washed 3x10 min in TTBS, still protected from light. The membrane was then ready to be scanned on the Odyssey system (LI-COR Biosciences). Electronic files of the gel image were analyzed using PaintShop program.

4.12 Real-Time PCR (RT-PCR)

Quantitative RT-PCR was performed in order to determine the gene expression of APC for each cell line. This method is used when one wants to simultaneously amplify and quantify the expression of a specific gene and is therefore also referred as qRT-PCR. When measuring the expression of a certain gene one looks at the messenger RNA (mRNA) level but in order to amplify the desired DNA sequence the mRNA has to be reverse transcribed to DNA using the enzyme reverse transcriptase. This DNA is also known as complementary DNA (cDNA) and only contains the exons and not the introns.

The qRT-PCR was performed on an ABI 7300 machine and the amplified DNA sequence was measured using fluorescence. SYBR Green is a DNA binding dye which fluoresces when it binds to double stranded DNA. This fluorescent probe only binds to the newly synthesized PCR products, thus the increase in the fluorescent signals parallels the generation of the PCR product and hence correlates to the amount of specific cDNA initially present in the sample. Total RNA was prepared from each cell line using RNeasy® Plus mini kit (Qiagen) according to manufacturers specifications. The High Capacity cDNA Reverse Transcription kit from Applied Biosystems (Foster City, United State) was used for the synthesis of cDNA according to manufacturers specifications. The forward and reverse primers (Table 7) were designed using Primer 3 software program. For the qRT-PCR reaction Power SYBR Green PCR Master Mix (Applied Biosystems) was employed. Each sample was set up in triplicates using the components and conditions shown in Table 10. The data was collected and analyzed by the computer software program ABI SDS version 1.4 using the ddCT method and as a housekeeping gene GAPDH was utilized for the normalization of the APC gene expression. This housekeeping gene is used as a standard or reference gene because it is expressed in all the cell lines and its expression is very similar in all, thus ensuring accuracy in the quantification. The relative gene expression of APC was calculated for the cell lines and the fluorescence was plotted against the qRT-PCR cycle number on a logarithmic scale where LIM 1215 was used as a calibrator (Figure 17).

Table 10. qRT-PCR scheme.

Components	**x1 (µl)**
2xMaster Mix	10
Forward primer [1 mM]	1
Reverse primer [1 mM]	1
cDNA [0.02 µg/µl]	5
DDW	3
Total volume	20

The qRT-PCR thermal cycling conditions used were:

50 °C 2 min
95 °C 10 min
[95 °C 0.15 min Tm_{opt} 1 min] x 40 cycles

The dissociation temperature was 95 °C and Tm_{opt} indicates the optimal annealing temperature for the primer which in this case was 60 °C.

5. Results

5.1 DNA sequencing

In this section I show the results of the sequencing graphs, the deduced DNA sequence and the corresponding protein sequences, derived using the *Editseq* program. The wt protein sequence is shown in black, and the mutated sequence is underlined and depicted in red, where dots show the stop of the protein. The different colours indicate the nucleotides; where blue is cytosine, red thymine, green adenine and black guanine.

5.1.1 B-Raf

I sequenced both exon 11 and exon 15 because they are reported to frequently harbour mutations. However, B-Raf mutations for the LIM cell lines were all found in exon 15, solely in codon 600 (GTG). The underlined letter in bold specifies the mutated nucleotide, also shown by an arrow in the affected cell line. The results, which were confirmed by reverse sequencing, show that the B-Raf mutations found in LIM 2408, 2537 and 2551 displayed the same T to A substitution (Figure 7B-D) leading to an amino acid substitution from V to E at codon 600 in exon 15 (Figure 7F). The other LIM cell lines displayed no mutations for B-Raf in this exon (data not shown). The wt DNA sequence is depicted in LIM 1215 (Figure 7A).

5.1.1.1 B-Raf exon 15

A. Wild type DNA sequence:

C T A G C T A C A G **T** G A A A T C T C G A T

LIM 1215 wt,wt

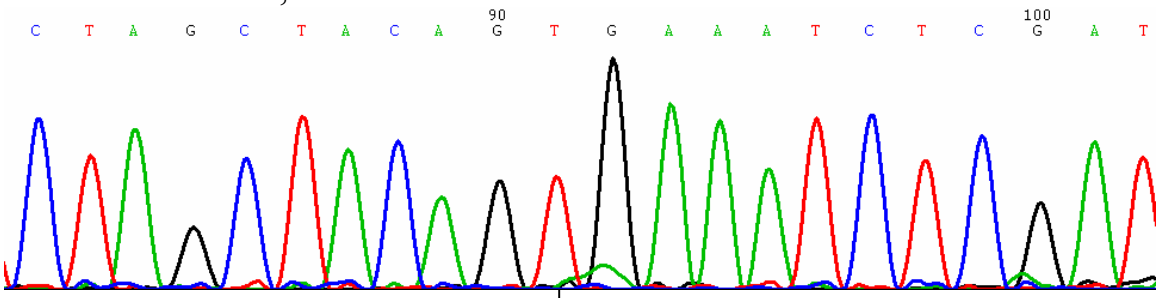

B. LIM 2408 mut, mut

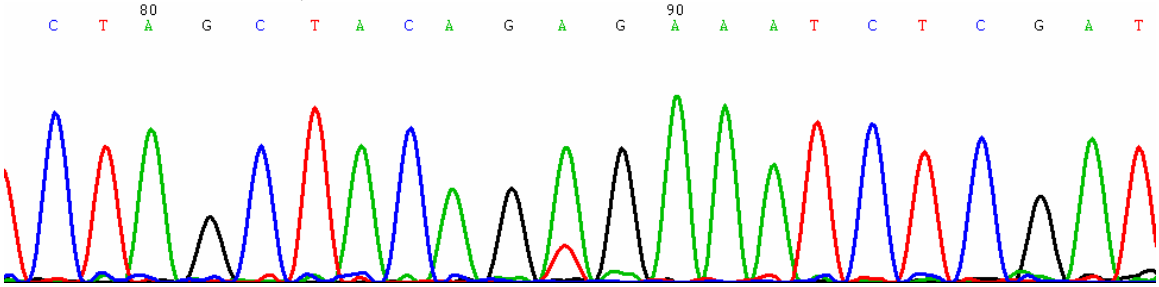

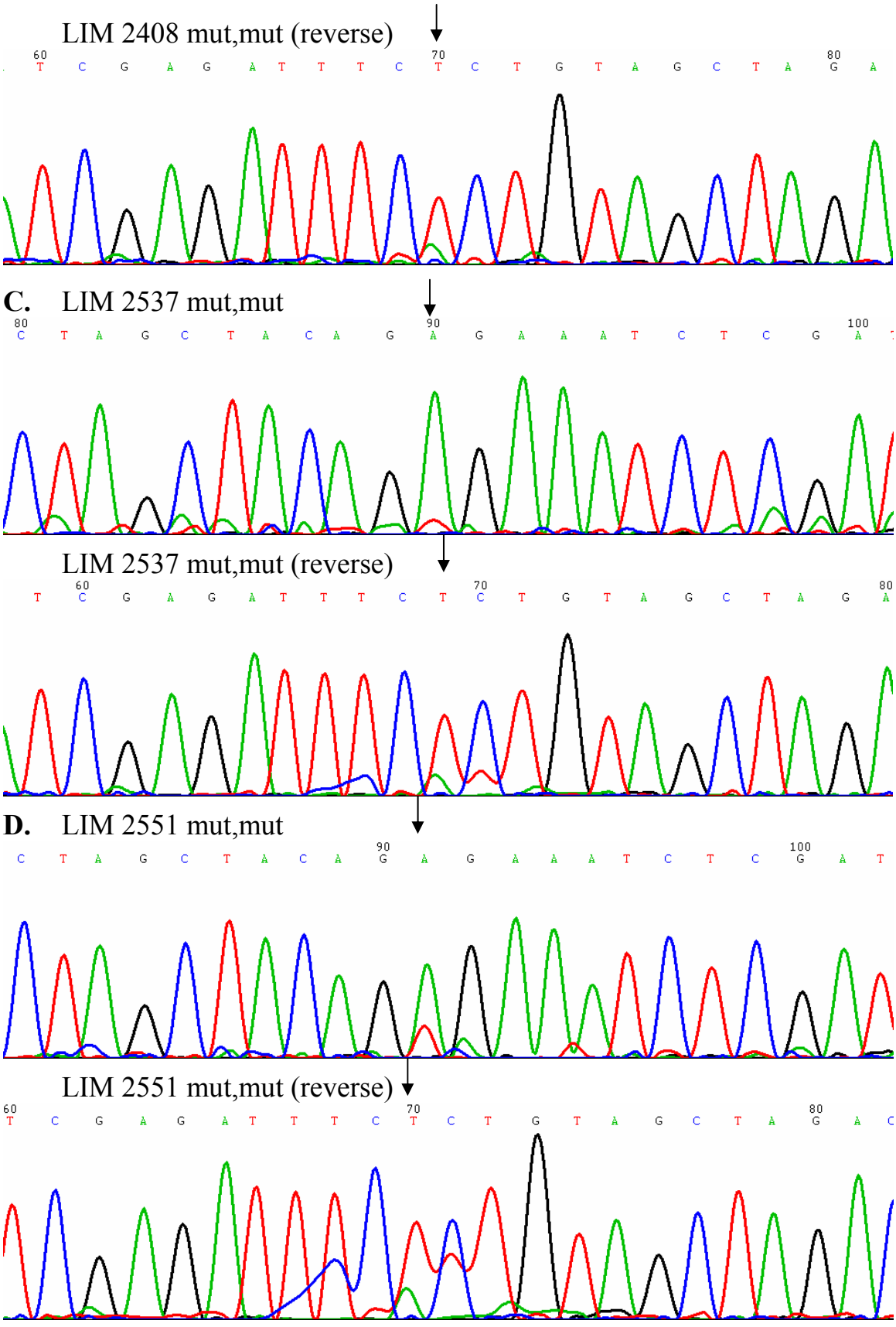
LIM 2408 mut,mut (reverse)
60
70
80
T C G A G A T T T C T C T G T A G C T A G A
C. LIM 2537 mut,mut
80
90
100
C T A G C T A C A G A G A A A T C T C G A T
LIM 2537 mut,mut (reverse)
60
70
80
T C G A G A T T T C T C T G T A G C T A G A
D. LIM 2551 mut,mut
90
100
C T A G C T A C A G A G A A A T C T C G A T
LIM 2551 mut,mut (reverse)
60
70
80
T C G A G A T T T C T C T G T A G C T A G A C

E. HT-29 wt,mut

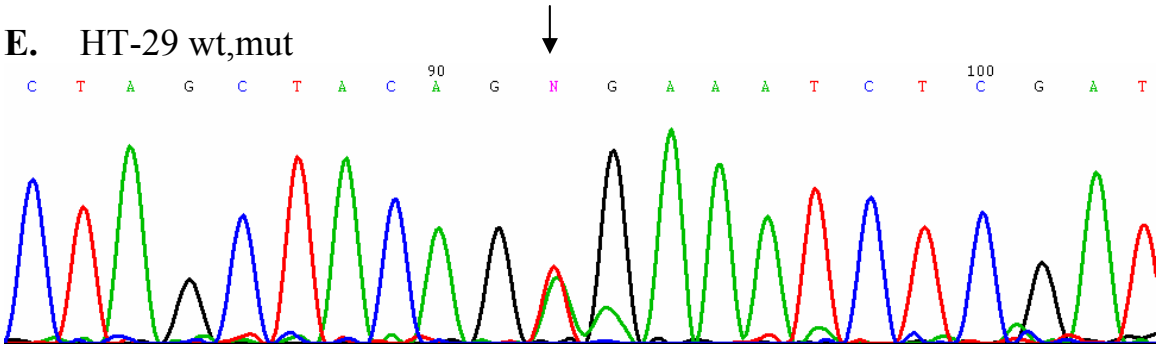

F.

Wild type protein sequence for exon 15 (aa 581-620):

IFLHEDLTVKIGDFGLATVKSRWSGSHQFEQLSGSILWM

Mutated protein sequence for exon 15 in LIM 2408, LIM 2537 and LIM 2551:

IFLHEDLTVKIGDFGLATEKSRWSGSHQFEQLSGSILWM

Figure 7. Sequence analysis of B-Raf exon 15. Genomic DNA was extracted from LIM cell lines and regions of interest were amplified using PCR, followed by sequencing of the purified PCR fragments. **A:** The wt DNA sequence derived from LIM 1215 cells. **B:** The forward and reverse sequences for LIM 2408 cells. **C:** The forward and reverse sequences for LIM 2537 cells. **D:** The forward and reverse sequences for LIM 2551 cells. **E:** Positive control for B-Raf mutation derived from HT-29 cells. **F:** The wild type B-Raf protein sequence for exon 15 (aa 581-620) compared to the detected mutated protein sequences for LIM 2408, 2537 and 2551. Arrows indicate the position of the mutations. The other LIM cell lines displayed no mutations for B-Raf in this exon (data not shown).

5.1.2 K-Ras

Codons 12 and 13 in exon 2 have been reported to harbour most of the K-Ras mutations but codon 61 in exon 3 also accounts for some mutations, I therefore I sequenced both. The underlined letters in bold specifies the mutated nucleotides, which are also shown by arrows in the affected cell lines.

5.1.2.1 K-Ras exon 2

The wild type DNA sequence is depicted in LIM 1215 (Figure 8A). Mutations in exon 2 occurred in either the first or the second G in codon 12 (GGT). For LIM 1899, a mutation in the second G was detected (Figure 8B) leading to a G to A amino acid substitution (Figure 8D), whereas for LIM 2099 the mutation occurred in the first G (Figure 8C) resulting in a G to C amino acid change (Figure 8D). All mutations were confirmed by reverse sequencing. The other LIM cell lines displayed no mutations for K-Ras in this exon (data not shown).

A. Wild type DNA sequence:

G T A G T T G G A G C T **G** **G** T G G C G T A G G

LIM 1215 wt,wt

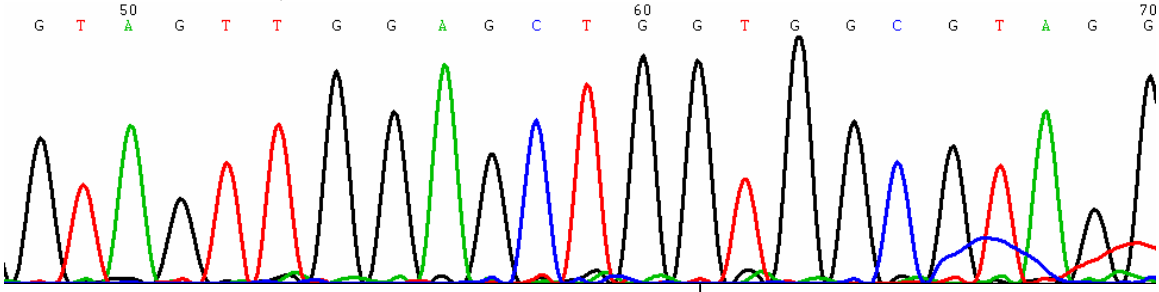

B. LIM 1899 wt,mut

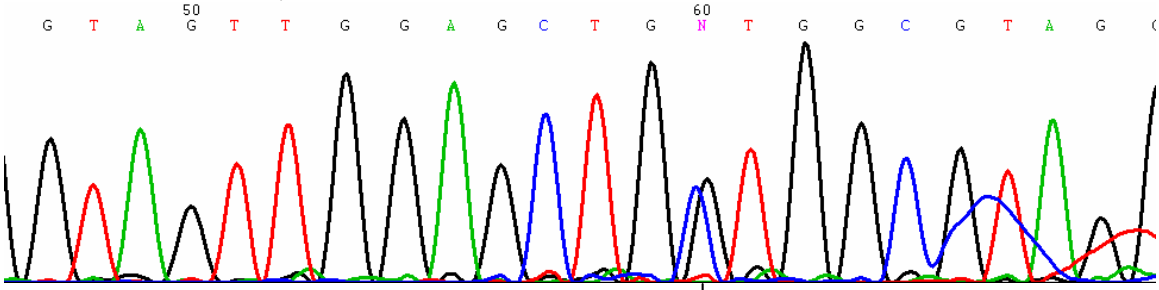

LIM 1899 wt,mut (reverse)

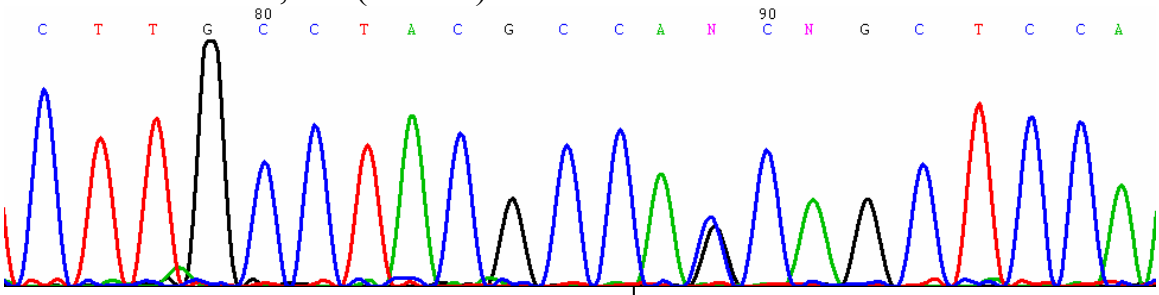

C. LIM 2099 mut,mut

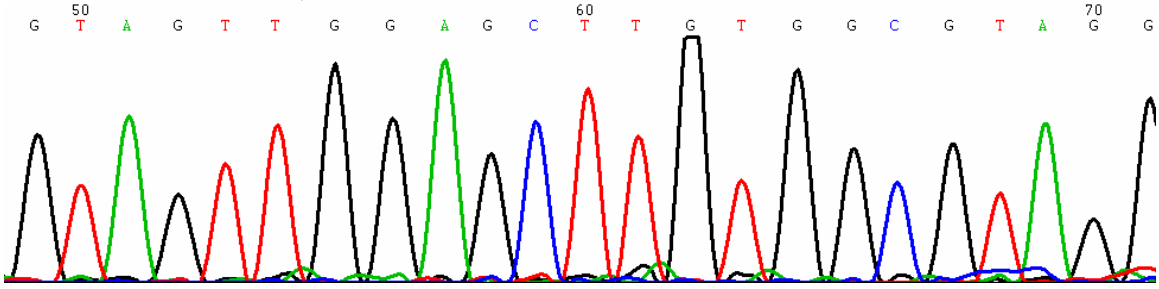

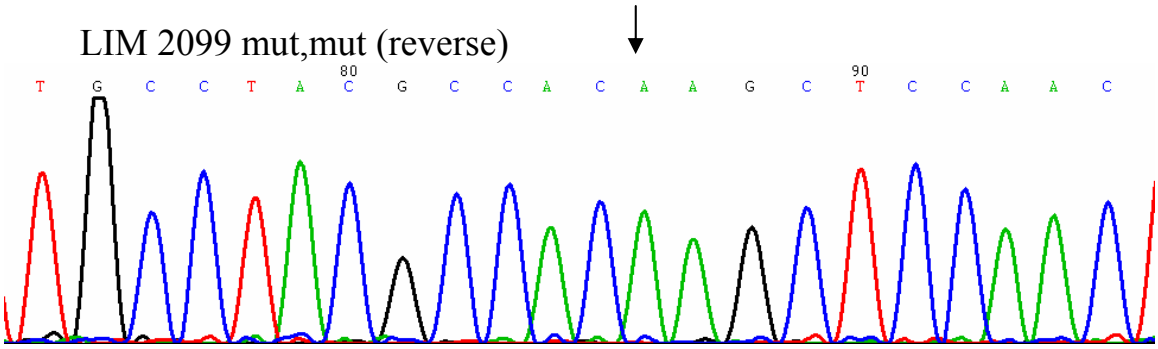

D.

Wild type protein sequence for exon 2 (aa 1-37):

MTEYKLVVVGAGGVGKSALTIQLIQNHFVDEYDPTIE

Mutated protein sequence for exon 2 in LIM 1899:

MTEYKLVVVGAAGVGKSALTIQLIQNHFVDEYDPTIE

Mutated protein sequence for exon 2 in LIM 2099:

MTEYKLVVVGACGVGKSALTIQLIQNHFVDEYDPTIE

Figure 8. Sequence analysis of K-Ras exon 2. Genomic DNA was extracted from LIM cell lines and regions of interest were amplified using PCR, followed by sequencing of the purified PCR fragments. **A:** The wt DNA sequence derived from LIM 1215 cells. **B:** The forward and reverse sequences for LIM 1899 cells. **C:** The forward and reverse sequences for LIM 2099 cells. **D:** The wild type K-Ras protein sequence for exon 2 (aa 1-37) compared to the detected mutated protein sequences in LIM 1899 and 2099. Arrows indicate the position of the mutations. The other LIM cell lines displayed no mutations for K-Ras in this exon (data not shown).

5.1.2.2 K-Ras exon 3

The wild type DNA sequence is depicted in LIM 1215 (Figure 9A). Mutations in exon 3 were detected in either C or A in codon 61 (CAA). LIM 2463 displayed an A to C change (Figure 9B) leading to a Q to H amino acid substitution (Figure 9D). In LIM 2550 the mutation resulted in a C to A change (Figure 9C) leading to an amino acid substitution from Q to K (Figure 9D). All mutations were confirmed by reverse sequencing. The other LIM cell lines displayed no mutations for K-Ras in this exon (data not shown).

A. Wild type DNA sequence:

A C A C A G C A G G T C A A G A G G A G T A C A

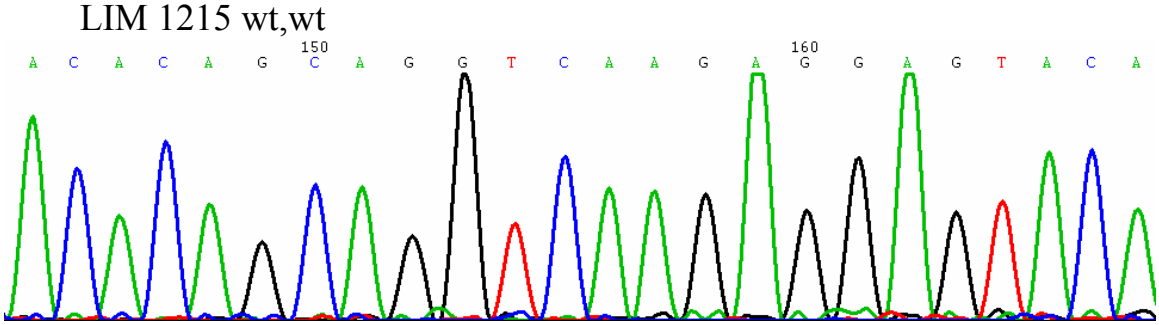

B. LIM 2463 wt,mut

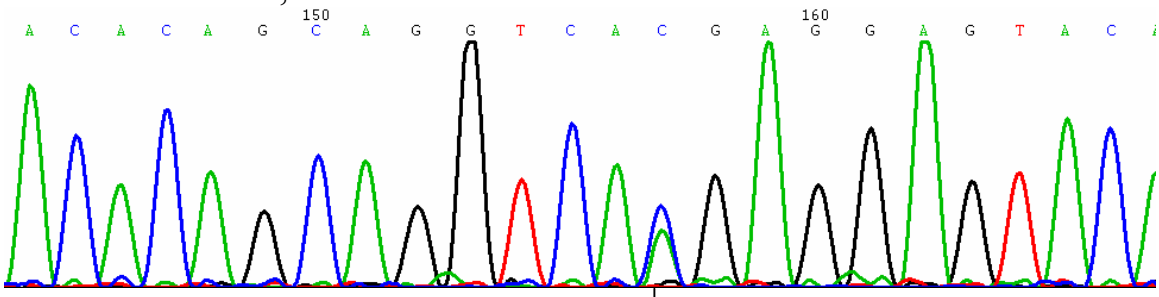

LIM 2463 wt,mut (reverse)

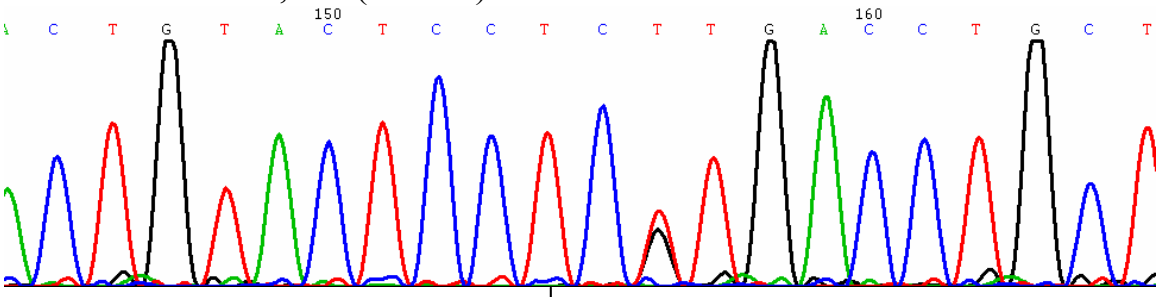

C. LIM 2550 wt,mut

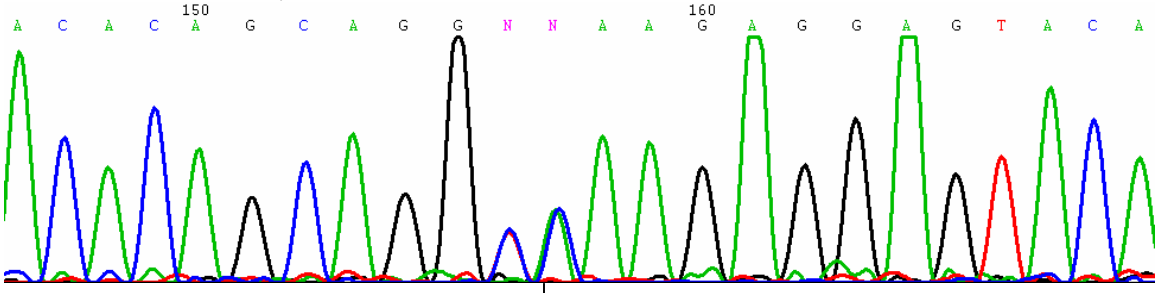

LIM 2550 wt,mut (reverse)

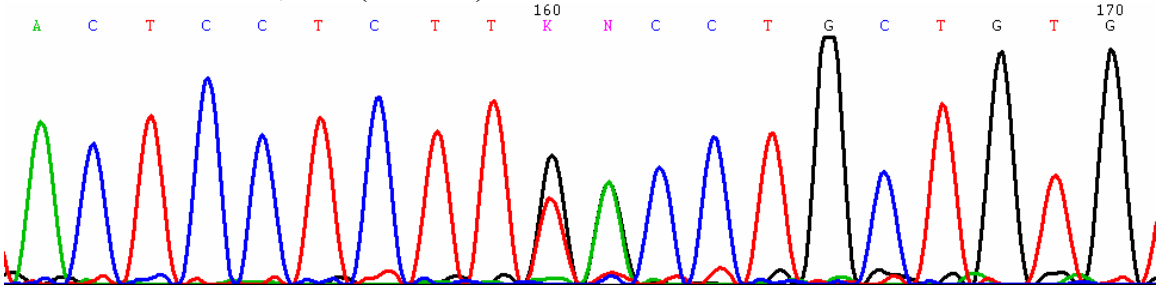

D.

Wild type protein sequence for exon 3 (aa 38-71):

DSYRKQVVIDGETCLLDILDTAGQEEYSAMRDQYMR

Mutated protein sequence for exon 3 in LIM 2463:

DSYRKQVVIDGETCLLDILDTAGHEEYSAMRDQYMR

Mutated protein sequence for exon 3 in LIM 2550:

DSYRKQVVIDGETCLLDILDTAGKEEYSAMRDQYMR

Figure 9. Sequence analysis of K-Ras exon 3. Genomic DNA was extracted from LIM cell lines and regions of interest were amplified using PCR, followed by sequencing of the purifired PCR fragments. **A:** The wt DNA sequence derived from LIM 1215 cells. **B:** The forward and reverse sequences for LIM 2463 cells. **C:** The forward and reverse sequences for LIM 2550 cells. **D:** The wild type K-Ras protein sequence for exon 3 (aa 38-71) compared to the detected mutated protein sequences in LIM 2463 and 2550. Arrows indicate the position of the mutations. The other LIM cell lines displayed no mutations for K-Ras in this exon (data not shown).

Table 11. Summary of B-Raf and K-Ras mutations in LIM cell lines. The amino acid substitutions and positions are shown within the brackets.

Cell line	B-Raf ex11	B-Raf ex15	K-Ras ex2	K-Ras ex3
1215	wt, wt	wt, wt	wt, wt	wt, wt
1863	wt, wt	wt, wt	wt, wt	wt, wt
1899	wt, wt	wt, wt	wt, **mut [G12A]**	wt, wt
2099	wt, wt	wt, wt	**Mut, mut [G12C]**	wt, wt
2408	wt, wt	**mut, mut [V600E]**	wt, wt	wt, wt
2463	wt, wt	wt, wt	wt, wt	wt, **mut [Q61H]**
2537	wt, wt	**mut, mut [V600E]**	wt, wt	wt, wt
2550	wt, wt	wt, wt	wt, wt	wt, **mut [Q61K]**
2551	wt, wt	**mut, mut [V600E]**	wt, wt	wt, wt

5.1.3 APC

The entire exon 16 comprises >75% of the coding sequence of the APC gene and harbours most of the mutations, therefore I started sequencing this exon. Sequencing of the other APC exons was performed only on cell lines which showed no mutations in exon 16. The underlined letter in bold specifies the mutated nucleotide, which is also shown by an arrow in the affected cell line.

A. Wild type DNA sequence:

G A T G C T G A T A C T T T A T T A C A T T T T

LIM 1215 wt,wt

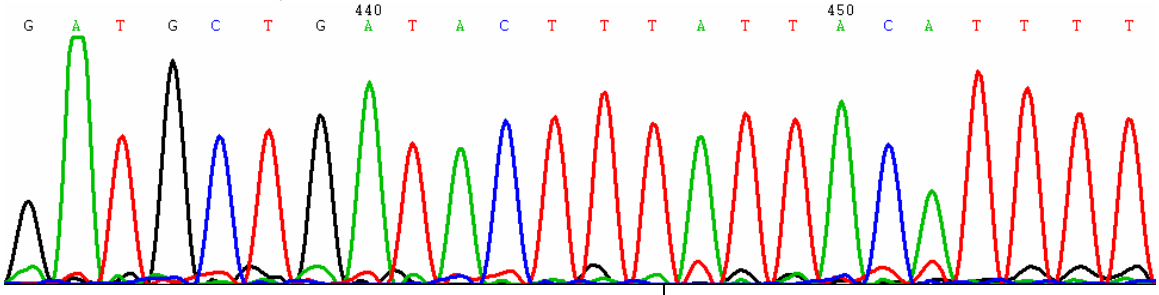

B. LIM 1863 mut,mut

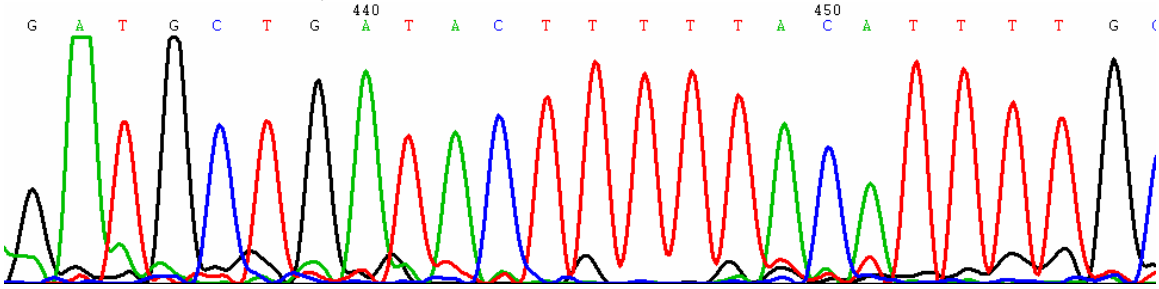

LIM 1863 mut,mut (subsequent overlapping primer)

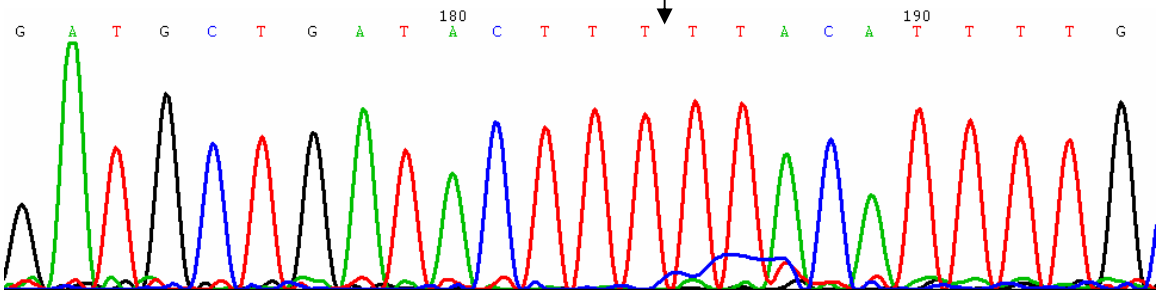

C.

Wild type protein sequence for exon 16 (aa 1477-1515):

…QRVQVLPDADTLLHFATESTPDGFSCSSSLSALSLDEPF…

Mutated protein sequence for exon 16 in LIM 1863:

…QRVQVLPDADTFYILPQKVLQMDFLVHPA.

Figure 10. Sequence analysis of APC exon 16. Genomic DNA was extracted from LIM cell lines and regions of interest were amplified using PCR, followed by sequencing of the purified PCR fragments. **A:** The wt DNA sequence derived from LIM 1215 cells. **B:** The forward and the overlapping primer sequences for LIM 1863 cells. **C:** The wild type APC protein sequence for exon 16 (aa 38-71) compared to the detected mutated protein sequence in LIM 1863. Arrows indicate the position of the mutations. The other LIM cell lines displayed no mutations for APC in this region of exon 16 (data not shown).

The wild type DNA sequence is depicted in LIM 1215 (Figure 10A). The mutation found in LIM 1863 displayed a deletion of an A (Figure 10B) in both alleles leading to a frame-shift in the DNA sequence, which resulted in a premature stop and a truncated protein (Figure 10C). The mutation was confirmed by sequencing with an overlapping primer (Figure 10B). The other LIM cell lines displayed no mutations for APC in this region of exon 16 (data not shown).

A. Wild type DNA sequence:

A A G G A G G A A A A A A A A G T T T A T A

LIM 1215 wt,wt

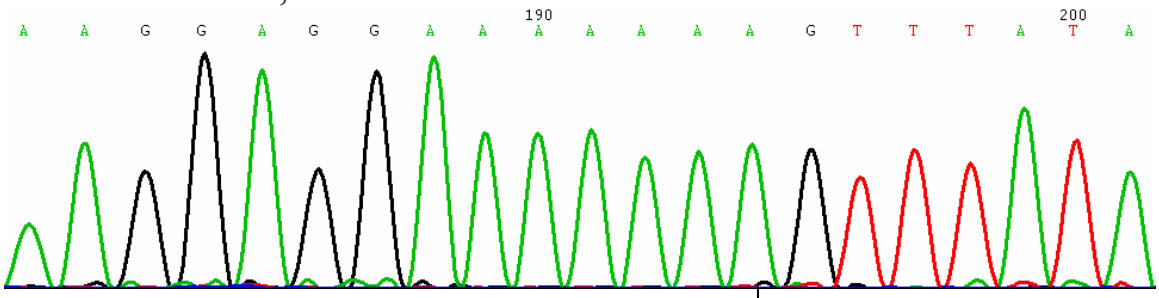

B. LIM 2408 wt,mut

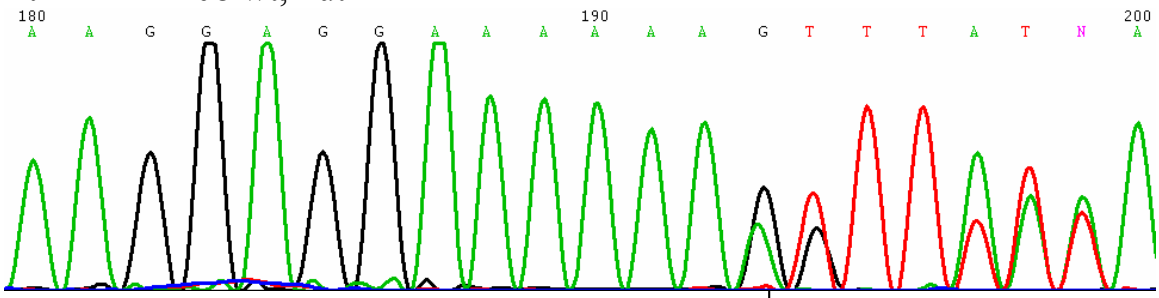

LIM 2408 wt,mut (reverse)

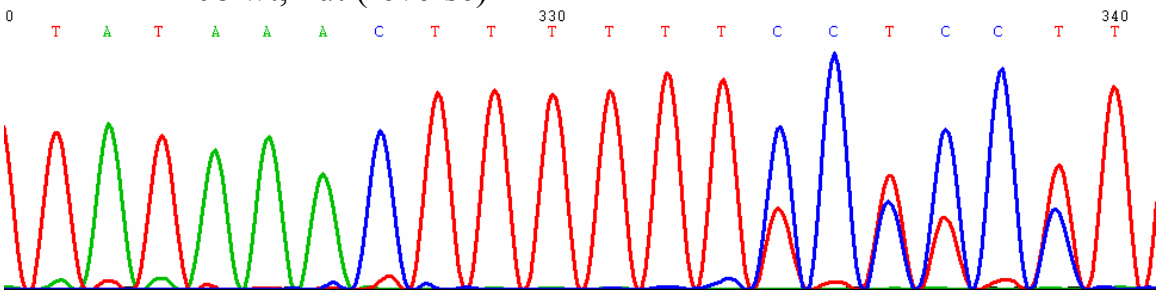

C.

Wild type protein sequence for exon 16 (aa 2165-2203):

…PRILKPGEKSTLETKKIESESKGIKGGKKVYKSLITGKV…

Mutated protein sequence for exon 16 in LIM 2408:

…PRILKPGEKSTLETKKIESESKGIKGGKKFIKV.

Figure 11. Sequence analysis of APC exon 16. Genomic DNA was extracted from LIM cell lines and regions of interest were amplified using PCR, followed by sequencing of the purified PCR fragments. **A:** The wt DNA sequence derived from LIM 1215 cells. **B:** The forward and reverse sequences for LIM 2408 cells. **C:** The wild type APC protein sequence for exon 16 (aa 2165-2203) compared to the detected mutated protein sequence in LIM 2408. Arrows indicate the position of the mutations. The other LIM cell lines displayed no mutations for APC in this region of exon 16 (data not shown).

The wild type DNA sequence is depicted in LIM 1215 (Figure 11A). The mutation found in LIM 2408 displayed a deletion of an A (Figure 11B) in one allele leading to a frame-shift in the DNA sequence, which resulted in a premature stop and a truncated protein (Figure 11C). The mutation was confirmed by reverse sequencing (Figure 11B). The other LIM cell lines displayed no mutations for APC in this region of exon 16 (data not shown).

A. Wild type DNA sequence:

A A A G A G A G A G A G T G G A C C T A A

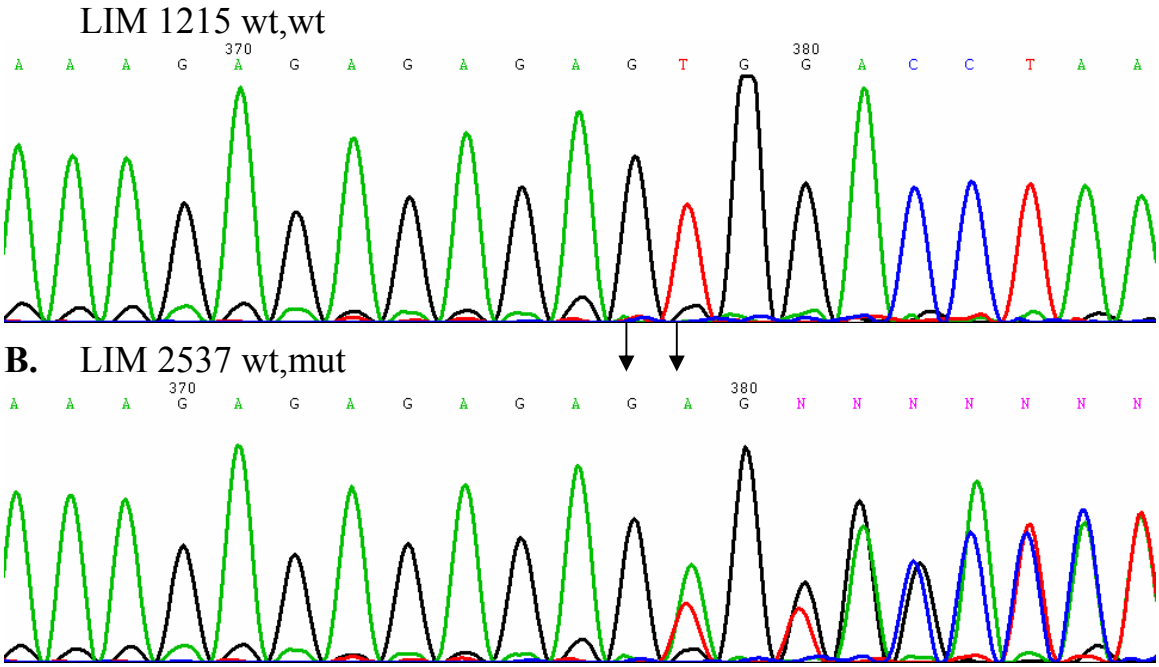

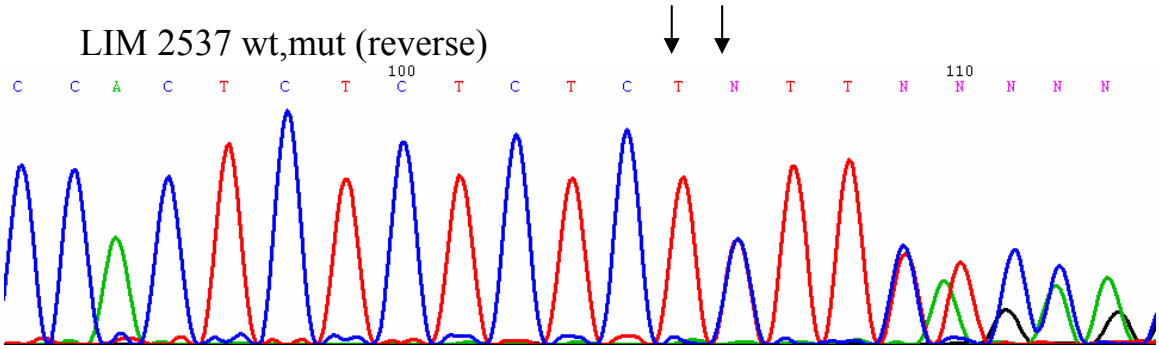

C.

Wild type protein sequence for exon 16 (aa 1447-1482):

…QTKREVPKNKAPTAEKRESGPKQAAVNAAVQRVQVL…

Mutated protein sequence for exon 16 in LIM 2537:

…QTKREVPKNKAPTAEKRERVDLSKLQ.

Figure 12. Sequence analysis of APC exon 16. Genomic DNA was extracted from LIM cell lines and regions of interest were amplified using PCR, followed by sequencing of the purified PCR fragments. **A:** The wt DNA sequence derived from LIM 1215 cells. **B:** The forward and reverse sequences for LIM 2537 cells. **C:** The wild type APC protein sequence for exon 16 (aa 1447-1482) compared to the detected mutated protein sequence in LIM 2537. Arrows indicate the position of the mutations. The other LIM cell lines displayed no mutations for APC in this region of exon 16 (data not shown).

The wild type DNA sequence is depicted in LIM 1215 (Figure 12A). The mutation found in LIM 2537 displayed an insertion of GA (Figure 12B) in one allele leading to a frame-shift in the DNA sequence that resulted in a premature stop and a truncated protein (Figure 12C). The mutation was confirmed by reverse sequencing (Figure 12B). The other LIM cell lines displayed no mutations for APC in this region of exon 16 (data not shown).

A. Wild type DNA sequence:

G C A G C C T A A A **G** A A T C A A A T G A

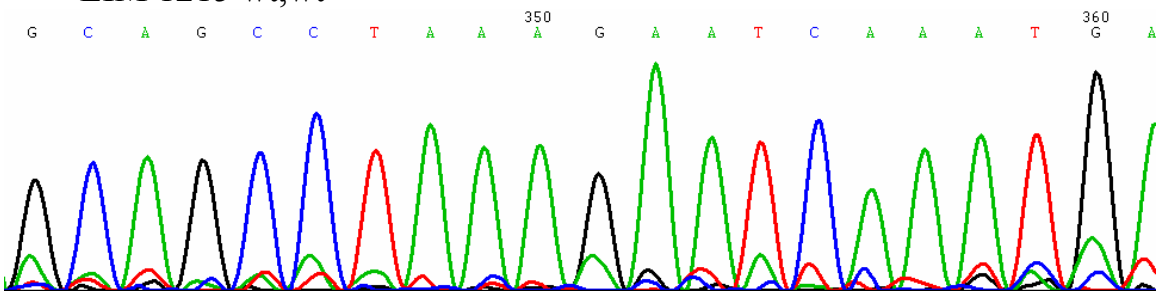

B. LIM 2550 mut,mut

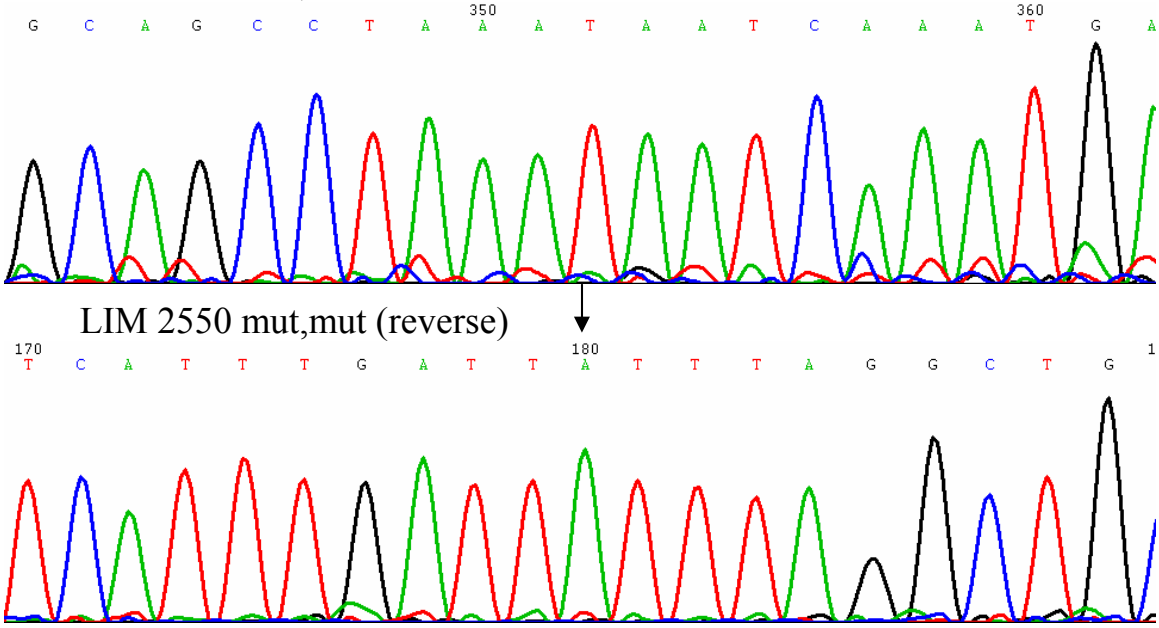

C.

Wild type protein sequence for exon 16 (aa 1512-1549):

…DEPFIQKDVELRIMPPVQENDNGNETESEQPKESNENQ…

Mutated protein sequence for exon 16 in LIM 2550:

…DEPFIQKDVELRIMPPVQENDNGNETESEQPK.

Figure 13. Sequence analysis of APC exon 16. Genomic DNA was extracted from LIM cell lines and regions of interest were amplified using PCR, followed by sequencing of the purified PCR fragments. **A:** The wt DNA sequence derived from LIM 1215 cells. **B:** The forward and reverse sequences for LIM 2550 cells. **C:** The wild type APC protein sequence for exon 16 (aa 1512-1549) compared to the detected mutated protein sequence in LIM 2550. Arrows indicate the position of the mutations. The other LIM cell lines displayed no mutations for APC in this region of exon 16 (data not shown).

The wild type DNA sequence is depicted in LIM 1215 (Figure 13A). The mutation found in LIM 2550 displayed a substitution of G to T (Figure 13B) in both alleles leading to a premature stop and a truncated protein (Figure 13C). The mutation was confirmed by reverse sequencing (Figure 13B). The other LIM cell lines displayed no mutations for APC in this region of exon 16 (data not shown).

Table 12. Summary of APC mutations in LIM cell lines. NA, not applicable; wt, wild type; del, deletion; aa, amino acid; ins, insertion; s.b. mut, single base mutation.

Cell line	Mutation status	Mutation in DNA sequence	Expected protein
1215	wt, wt	NA	wt
1863	**mut ***	del of A in codon 1488	stop at aa 1506
1899	wt, wt	NA	wt
2099	wt, wt	NA	wt
2408	wt, **mut**	del of A in codon 2193	stop at aa 2198
2463	wt, wt	NA	wt
2537	wt, **mut**	ins of GA in codon 1465	stop at aa 1472
2550	**mut ***	s.b. mut G -> T in codon 1544	stop at aa 1544
2551	wt, wt	NA	wt

* where only the mutated form of APC was detected, it is impossible to discriminate between homozygous mutation and loss of heterozygosity (LOH).

5.1.4 TGFβRII microsatellite

In the TGFβ receptor type II gene, microsatellite instability most often causes mutations in the sequence AAAAAAAAAA (codon 125-128 in exon 3). Therefore I concentrated on this exon for sequencing.

A. Wild type DNA sequence:

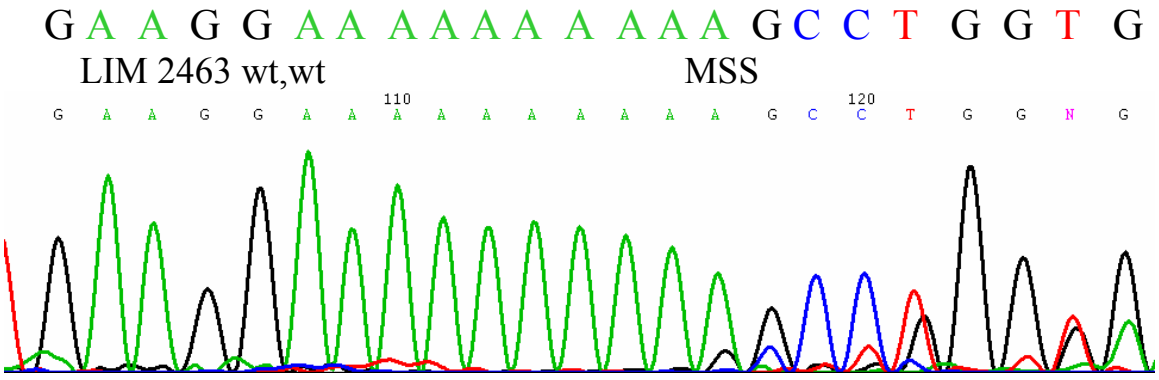

B. LIM 1215 -1,-1 MSI

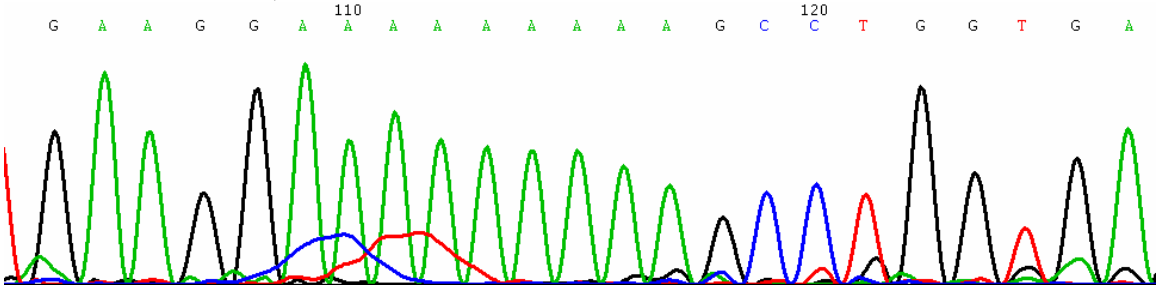

LIM 1215 -1,-1 (reverse) MSI

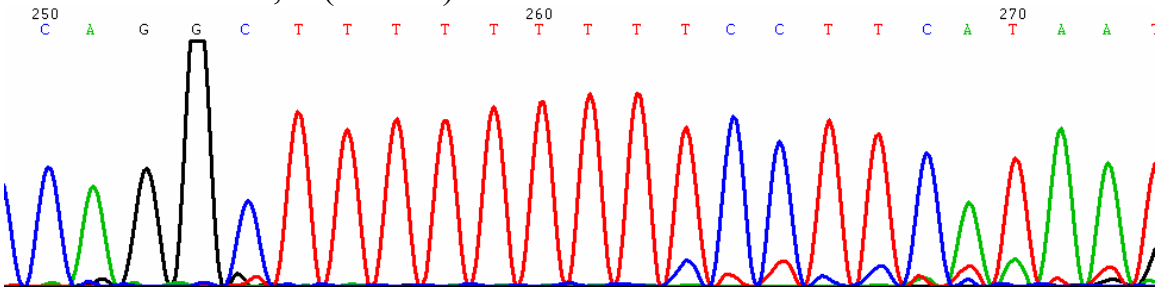

C. LIM 1899 -2,+1 MSS

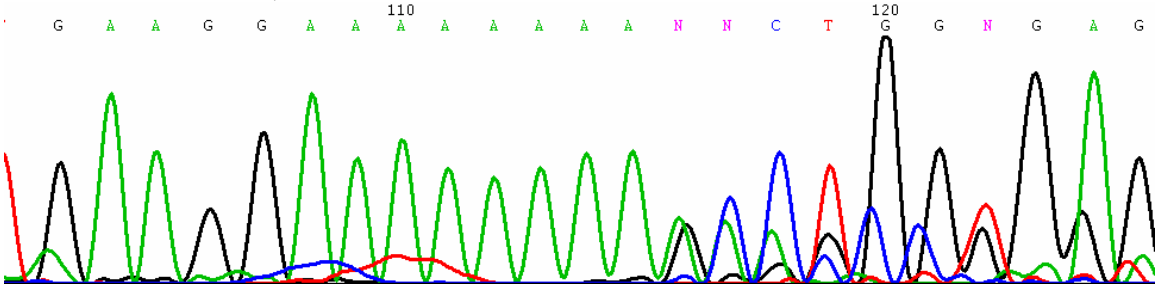

LIM 1899 -2,+1 (reverse) MSS

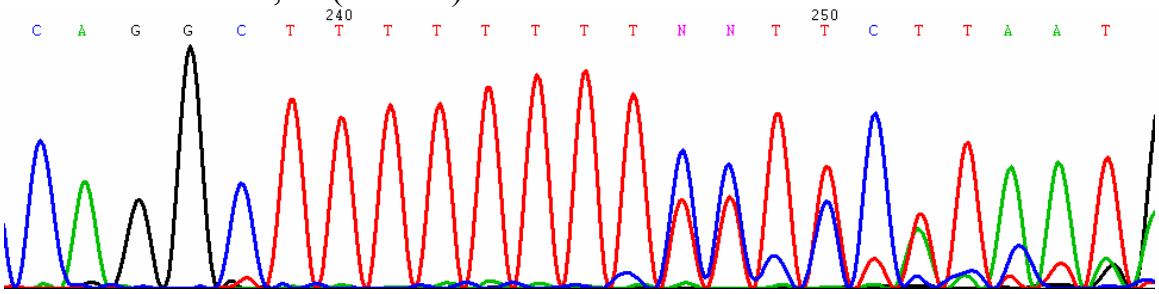

D. LIM 2537 -1,-2 MSI

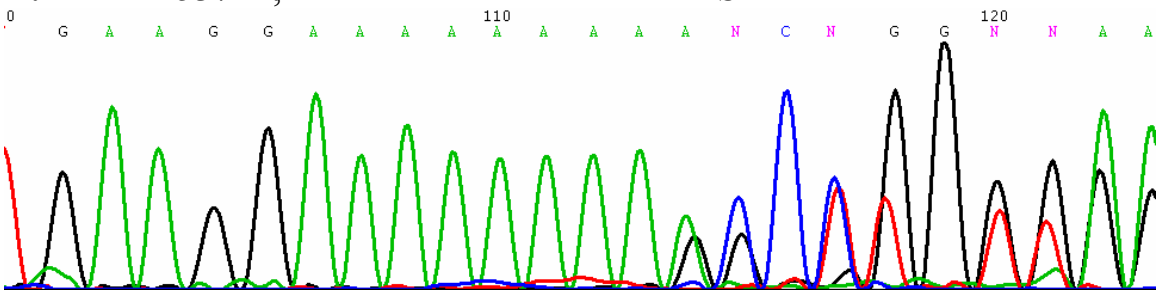

LIM 2537 -1,-2 (reverse) MSI

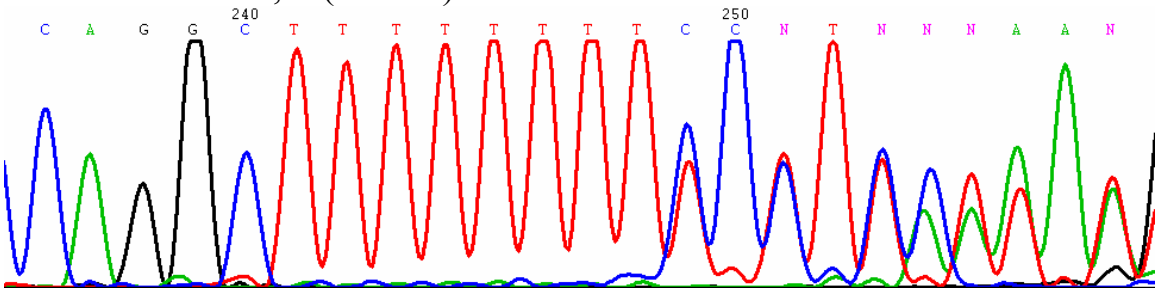

E. LIM 2550 -1,wt MSI

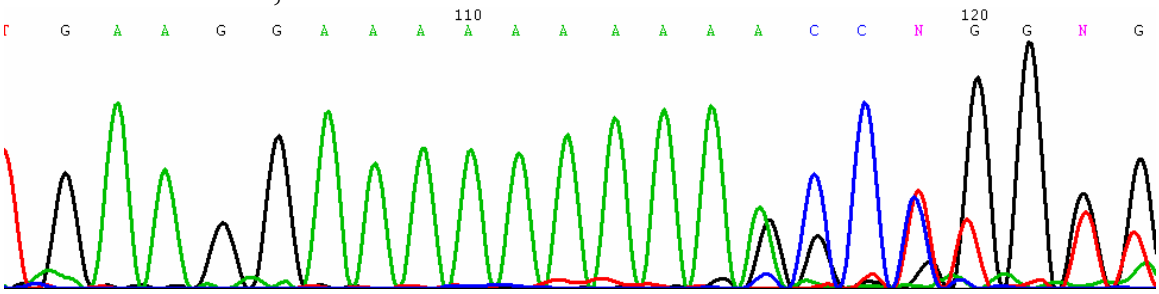

LIM 2550 -1,wt (reverse) MSI

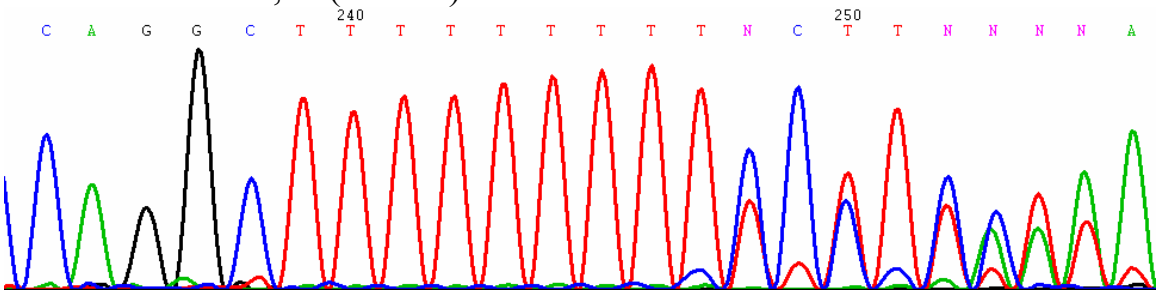

F. LIM 2551 -1,-1 MSI

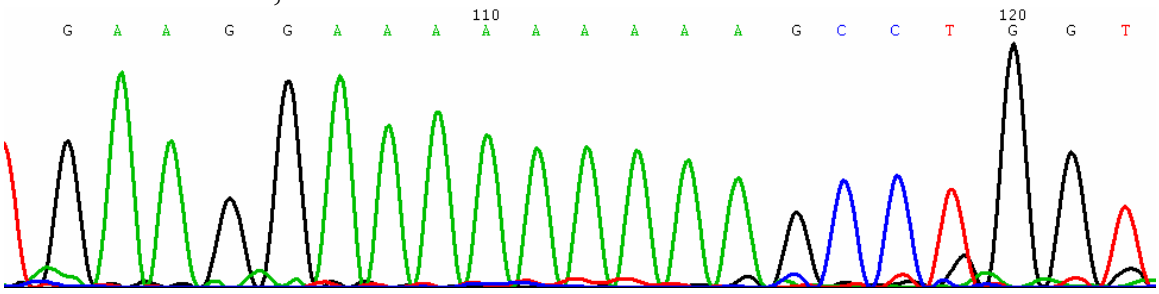

LIM 2551 -1,-1 (reverse) MSI

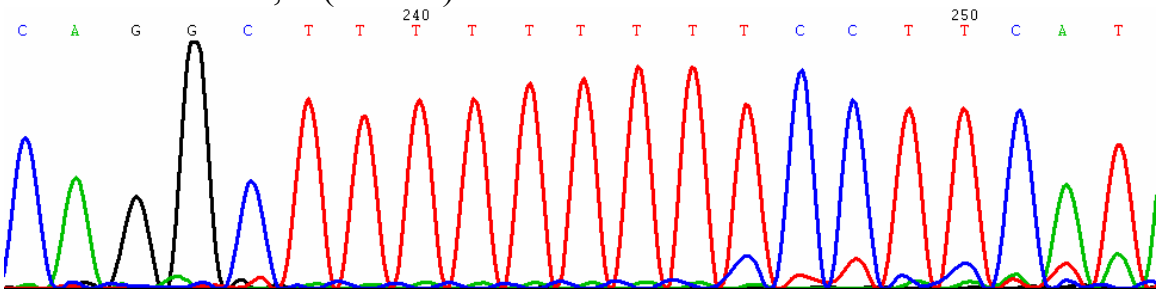

G.

Wild type protein sequence for exon 3 (aa 93-151):

RKNDENITLETVCHDPKLPYHDFILEDAASPKCIMKEKKKP
GETFFMCSCSSDECNDNIIFSE

Mutated protein sequence for -1 frame-shift in exon 3 in LIM 1215:

RKNDENITLETVCHDPKLPYHDFILEDAASPKCIMKEKKSL
VRLSSCVPVALMSAMTTSSSQK

Mutated protein sequence for -2 frame-shift in exon 3 in LIM 1899:

RKNDENITLETVCHDPKLPYHDFILEDAASPKCIMKEKKAW

Mutated protein sequence for +1 frame-shift in exon 3 in LIM 1899:

RKNDENITLETVCHDPKLPYHDFILEDAASPKCIMKEKKKA
W

Mutated protein sequence for -1 frame-shift in exon 3 in LIM 2537:

RKNDENITLETVCHDPKLPYHDFILEDAASPKCIMKEKKSL
VRLSSCVPVALMSAMTTSSSQK

Mutated protein sequence for -2 frame-shift in exon 3 in LIM 2537:

RKNDENITLETVCHDPKLPYHDFILEDAASPKCIMKEKKAW

Mutated protein sequence for -1 frame-shift in exon 3 in LIM 2550:

RKNDENITLETVCHDPKLPYHDFILEDAASPKCIMKEKKSL
VRLSSCVPVALMSAMTTSSSQK

Mutated protein sequence for -1 frame-shift in exon 3 in LIM 2551:

RKNDENITLETVCHDPKLPYHDFILEDAASPKCIMKEKKSL
VRLSSCVPVALMSAMTTSSSQK

Figure 14. Sequence analysis of TGFβRII exon 3. Genomic DNA was extracted from LIM cell lines and regions of interest were amplified using PCR, followed by sequencing of the purified PCR fragments. **A:** The wt DNA sequence derived from LIM 2463 cells. **B:** The forward and reverse sequences for LIM 1215 cells. **C:** The forward and reverse sequences for LIM 1899 cells. **D:** The forward and reverse sequences for LIM 2537 cells. **E:** The forward and reverse sequences for LIM 2550 cells. **F:** The forward and reverse sequences for LIM 2551 cells. **G:** The wild type TGFβRII protein sequence for exon 3 (aa 93-151) compared to the detected mutated protein sequences in LIM 1215, 1899, 2537, 2550 and 2551. Arrows indicate the position of the mutations. The other LIM cell lines displayed no mutations for TGFβRII in this exon (data not shown). MSS, microsatellite stable; MSI, microsatellite unstable.

The wild type DNA sequence is depicted in LIM 2463 (Figure 14A). The mutation found in LIM 1215 displayed a deletion of an A in both alleles (Figure 14B) leading to a frame-shift in the DNA sequence and therefore an altered amino acid sequence (Figure 14G). LIM 1899 demonstrated a deletion of two A's in one allele and an insertion of an A in the other (Figure 14C) leading to frame-shifts and altered amino acid sequences (Figure 14G). In LIM 2537 deletions of an A in one allele and two A's in the other (Figure 14D) resulted in frame-shifts and altered amino acid sequences (Figure 14G). The mutation in LIM 2550 displayed a deletion of an A in one allele (Figure 14E) leading to a frame-shift

in the DNA sequence and therefore an altered amino acid sequence (Figure 14G). LIM 2551 showed a deletion of an A in both alleles (Figure 14F) resulting in a frame-shift and an altered amino acid sequence (Figure 14G). All mutations were confirmed by reverse sequencing. The other LIM cell lines displayed no mutations for TGFβRII in exon 3 (data not shown).

5.1.5 BAX microsatellite

In the BAX gene, microsatellite instability most often causes mutations in the sequence GGGGGGGG which is found at codon 38-41 in exon 3. Therefore I concentrated on this exon for sequencing. Due to time constraint, only six of the nine cell lines have been characterized for mutations in the BAX gene.

A. Wild type DNA sequence:

G C G A A T G G G G G G G G A G G C A C

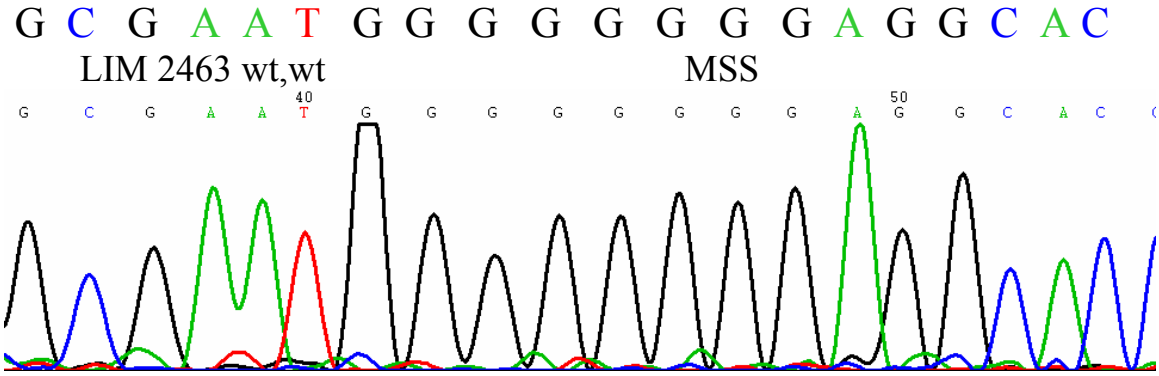

B. 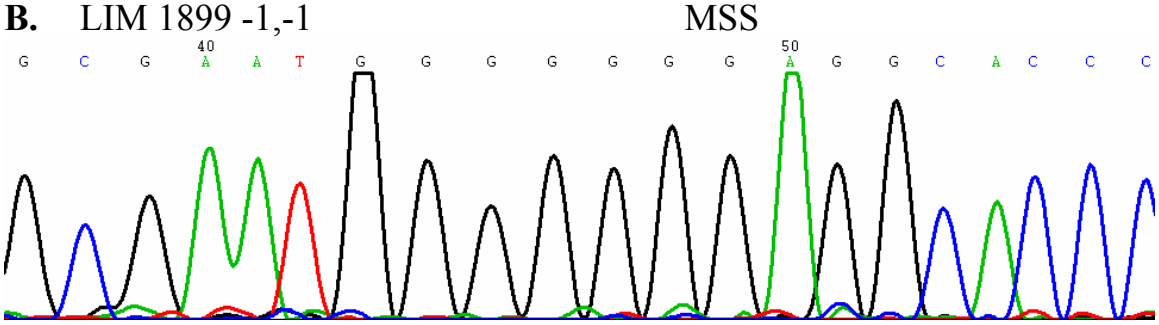

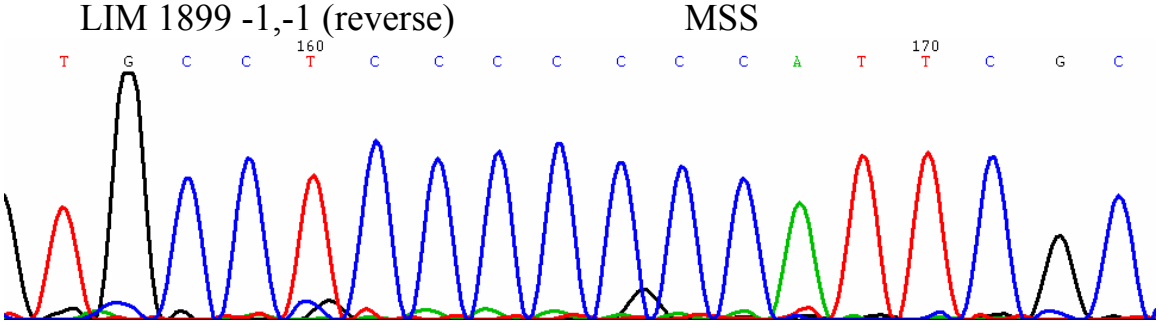

C. LIM 2537 -1,wt MSI

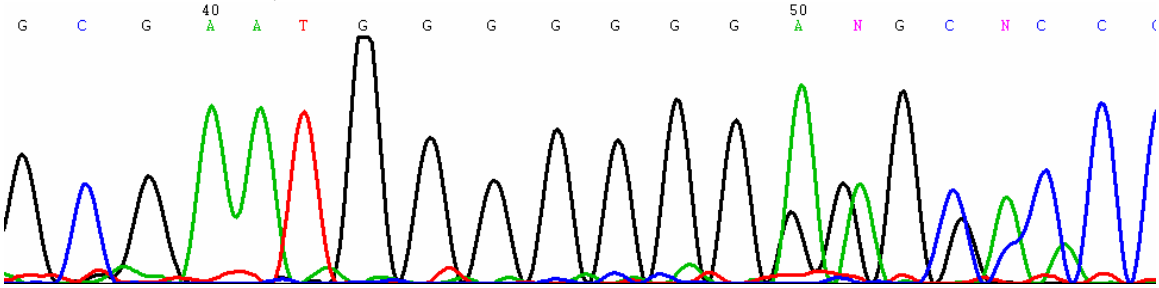

LIM 2537 -1,wt (reverse) MSI

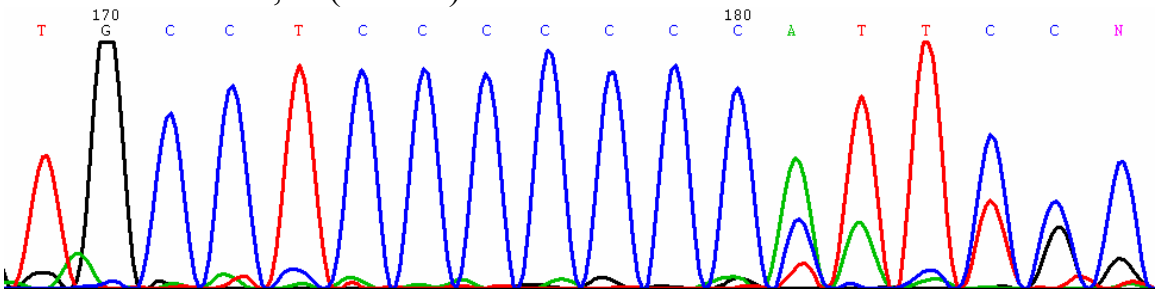

D.

Wild type protein sequence for exon 3 (aa 30-77):

FIQDRAGRMGGEAPELALDPVPQDASTKKLSECLKRIGDEL DSNMELQ

Mutated protein sequence for -1 frame-shift in exon 3 in LIM 1899:

FIQDRAGRMGGRHPSWPWTRCLRMRPPRS.

Mutated protein sequence for -1 frame-shift in exon 3 in LIM 2537:

FIQDRAGRMGGRHPSWPWTRCLRMRPPRS.

Figure 15. Sequence analysis of BAX exon 3. Genomic DNA was extracted from LIM cell lines and regions of interest were amplified using PCR, followed by sequencing of the purified PCR fragments. **A:** The wt DNA sequence derived from LIM 2463 cells. **B:** The forward and reverse sequences for LIM 1899 cells. **C:** The forward and reverse sequences for LIM 2537 cells. **D:** The wild type BAX protein sequence for exon 3 (aa 30-77) compared to the detected mutated protein sequences in LIM 1899 and 2537. Arrows indicate the position of the mutations. The other LIM cell lines displayed no mutations for BAX in this exon (data not shown). MSS, microsatellite stable; MSI, microsatellite unstable.

The wild type DNA sequence is depicted in LIM 2463 (Figure 15A). The mutation found in LIM 1899 displayed a deletion of a G in both alleles (Figure 15B) leading to a frame-shift in the DNA sequence resulting in an altered amino acid sequence (Figure 15D). LIM 2537 demonstrated a deletion of a G in one allele (Figure 15C) leading to a frame-shift and an altered amino acid sequence (Figure 15D). Both mutations were confirmed by reverse sequencing (Figure 15B-C). The other LIM cell lines displayed no mutations for BAX in exon 3 (data not shown).

Table 13. Summary of TGFβRII and BAX mutations in LIM cell lines. NA, not applicable; MSI, microsatellite unstable; MSS, microsatellite stable.

Cell line	Microsatellite status	TGFβRII micro	TGFβRII premature stop in ex4	BAX
1215	MSI	**-1, -1**	Yes	NA
1863	MSS	wt, wt	No	NA
1899	MSS	**-2,+1**	NA	**-1, -1**
2099	MSS	wt, wt	No	NA
2408	MSI	wt, wt	No	wt, wt
2463	MSS	wt, wt	No	wt, wt
2537	MSI	**-1, -2**	Yes	**-1,** wt
2550	MSI	**-1,** wt	Yes	wt, wt
2551	MSI	**-1, -1**	Yes	wt, wt

5.2 Western blot for APC

Immunodetection of APC protein was performed to confirm the presence of the wt or mutated APC protein.

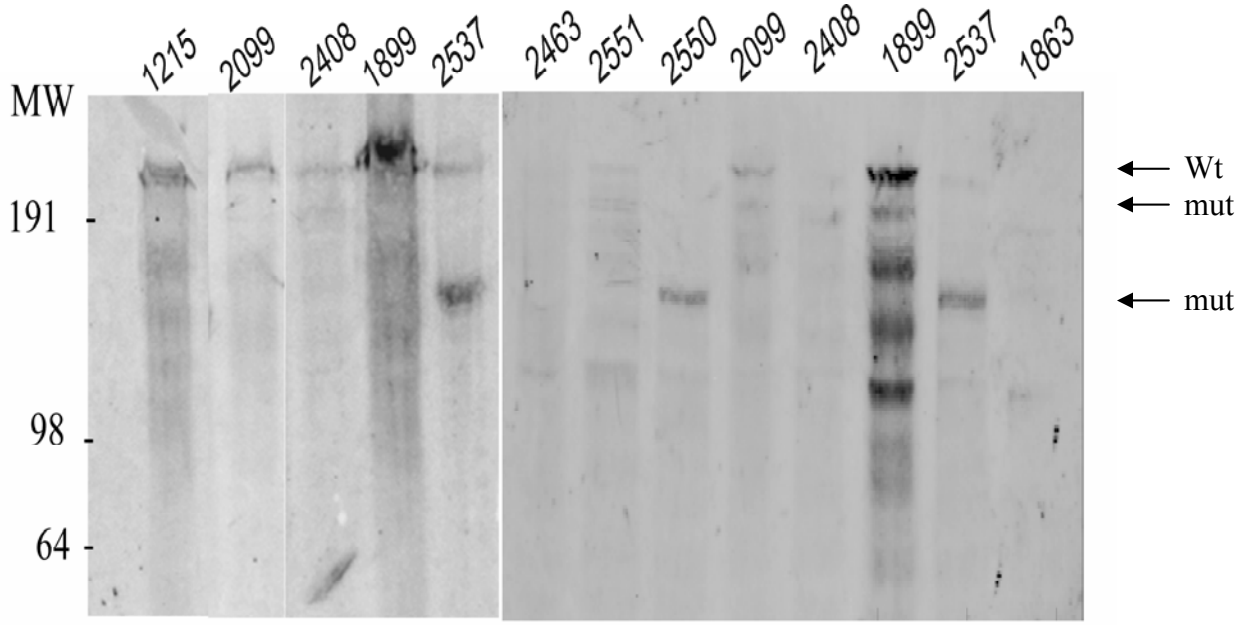

Figure 16. Western blot analysis of APC in LIM cell lines. Western blotting was performed using the H-290 antibody on total cell lysates. Equal amounts of protein were loaded per lane. Because results from two different experiments are shown some cell lines are in duplicate. Wt APC bands (312 kDa) were detected in LIM 1215, 1899, 2099, 2408 and 2537. Truncated bands were seen in LIM 2408, 2537, 2550 and barely in 1863, while no bands could be detected in LIM 2463 and 2551. Numbers at left are MW in kilodaltons. Wt, wild type; mut, mutation.

Results are shown from two different experiments, hence the duplicate results for some of the cell lines. Wild type bands (apparent MW of 312 kDa) could be seen for LIM 1215, LIM 1899 and LIM 2099, but also for LIM 2408 and LIM 2537 which showed heterozygous mutations in APC. Truncated bands were visible for LIM 2408, 2537 and 2550 while for LIM 1863 the truncated band was barely visible: this could be due to a low quality of the Rabbit anti-APC antibody (H-290) or to low gene expression of APC (Figure 17). The mutation detected by sequencing however is consistent with the observed molecular weight. No specific APC-reactive bands were detected for LIM 2463 and LIM 2551 in the numerous Western blots that were conducted. It was postulated that expression of APC may be very low in these cell lines, and this was verified by qRT-PCR. All cell lines except LIM 2550 showed a lower APC expression when compared to LIM 1215 which was used as a calibrator; LIM 1863, 2463 and 2551 had the lowest APC levels of all, and the message for APC was barely detectable in LIM 2463 (Figure 17). These results explain why I consistently failed to detect APC at the protein level in this cell line.

5.3 Gene expression of APC

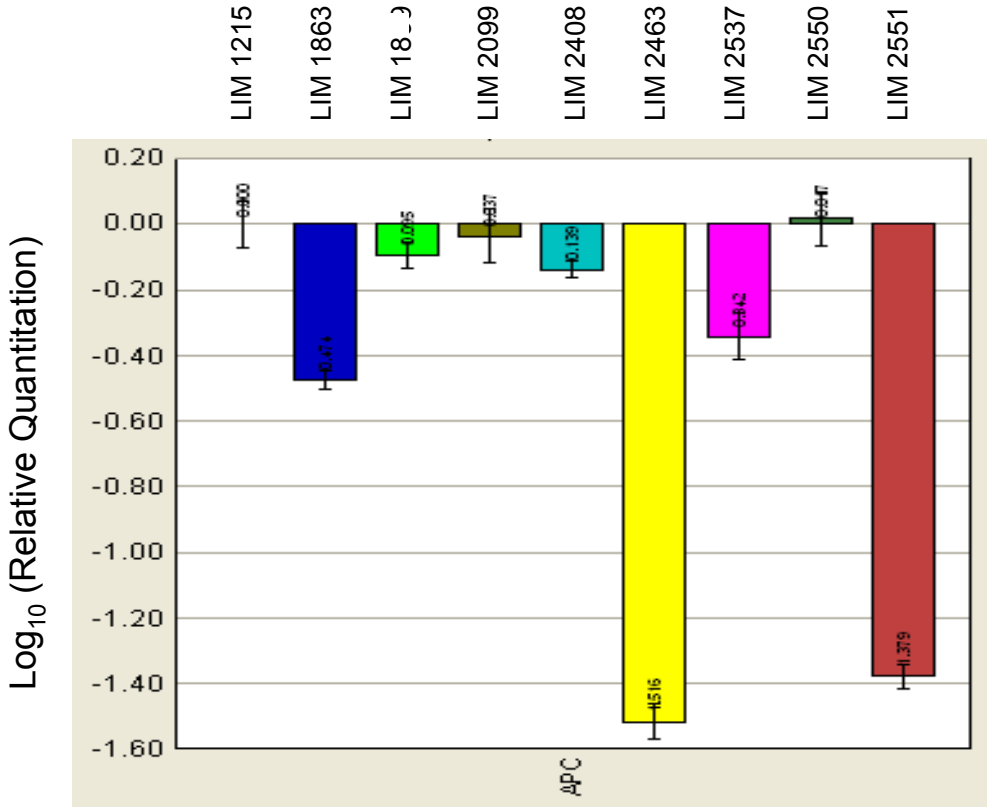

Figure 17. Gene expression of APC for LIM cell lines. Total RNA was prepared from LIM cell lines and used for synthesis of cDNA. Specific sequences were amplified using qRT-PCR. The relative gene expression of APC for each cell line was calculated using the computer software program ABI SDS version 1.4 and the data was plotted on a logarithmic scale. LIM 1215 was used as a calibrator.

Table 14. Summary of mutations in LIM cell lines.

Cell line	TGFβRII micro	BAX	B-Raf ex11	B-Raf ex15	K-Ras ex2	K-Ras ex3	APC
1215	**mut, mut**	NA	wt, wt	wt, wt	wt, wt	wt, wt	wt, wt
1863	wt, wt	NA	wt, wt	wt, wt	wt, wt	wt, wt	**mut ***
1899	**mut, mut**	**mut, mut**	wt, wt	wt, wt	wt, **mut**	wt, wt	wt, wt
2099	wt, wt	NA	wt, wt	wt, wt	**mut, mut**	wt, wt	wt, wt
2408	wt, wt	wt, wt	wt, wt	**mut, mut**	wt, wt	wt, wt	wt, **mut**
2463	wt, wt	wt, wt	wt, wt	wt, wt	wt, wt	wt, **mut**	wt, wt
2537	**mut, mut**	wt, **mut**	wt, wt	**mut, mut**	wt, wt	wt, wt	wt, **mut**
2550	wt, **mut**	wt, wt	wt, wt	wt, wt	wt, wt	wt, **mut**	**mut ***
2551	**mut, mut**	wt, wt	wt, wt	**mut, mut**	wt, wt	wt, wt	wt, wt

* either homozygous mutation or LOH.

6. Discussion

6.1 The ERK-MAPK pathway

The ERK-MAPK pathway is essential for the transmittance of signals controlling growth and differentiation from the cell surface growth factor receptors to the nucleus. The two key regulators of this pathway are the Ras and Raf proteins. Mutations at specific serine and threonine residues in either Ras or Raf lead to constitutive activation, which bypasses the need for extracellular-signal mediated activation and mimics the positive regulation of cell proliferation by growth factors and cytokines.

The activating mutations in the Ras protein predominantly occur in codon 12 (GGT) and in codon 13 (GGC), but they have also been found in codons 19 (TTG) and 61 (CAA). Codons 12 and 13 form part of the GTP/GDP-binding domain and codon 61 is in the GTPase domain (Figure 2). Mutations at both codon 12 and 61 interfere with GAP function, preventing it from assuming the correct structure for hydrolysis of GTP to GDP, resulting in a "locked" active state and the constitutive activation of the ERK-MAPK pathway.

The most common activating mutation in Raf occurs at codon 600, where a valine has been substituted for a glutamic acid, which results in an elevated kinase activity of Raf and the constitutive activation of the ERK-MAPK pathway independent of Ras. The V600E mutation takes place in the activation segment which is adjacent to the conserved DFG (aspartic acid, phenylalanine and glycine) motif. This will destabilize the inactive conformation of the DFG motif/activation segment resulting in a conversion of the activation segment into the active state, thereby mimicking the transient phosphorylation of Thr599 and Ser602, which occurs during normal signalling.

Mutations in Ras and Raf are mutually exclusive meaning that mutations in both Ras and Raf are rarely found in the same tumour sample, which is confirmed by the results in Table 14. LIM cell lines 2408, 2537 and 2551 displayed a V600E mutation in B-Raf and furthermore, LIM 2408 and 2537 showed additional mutations in APC. K-Ras mutations were observed in codon 12 for LIM 1899 and 2099 and in codon 61 for LIM 2463 and 2550, which also displayed a mutation in APC (Table 11 and Table 14).

According to the literature there is a correlation between the Wnt and the ERK-MAPK signalling pathways as they both promote cell growth. This correlation can to some extent be verified by the results obtained in this project (see below), but further analysis of mutations in other components in Wnt signalling pathway, such as β-catenin, must be performed before any definite conclusions about the relationship can be made.

6.2 Truncated APC proteins

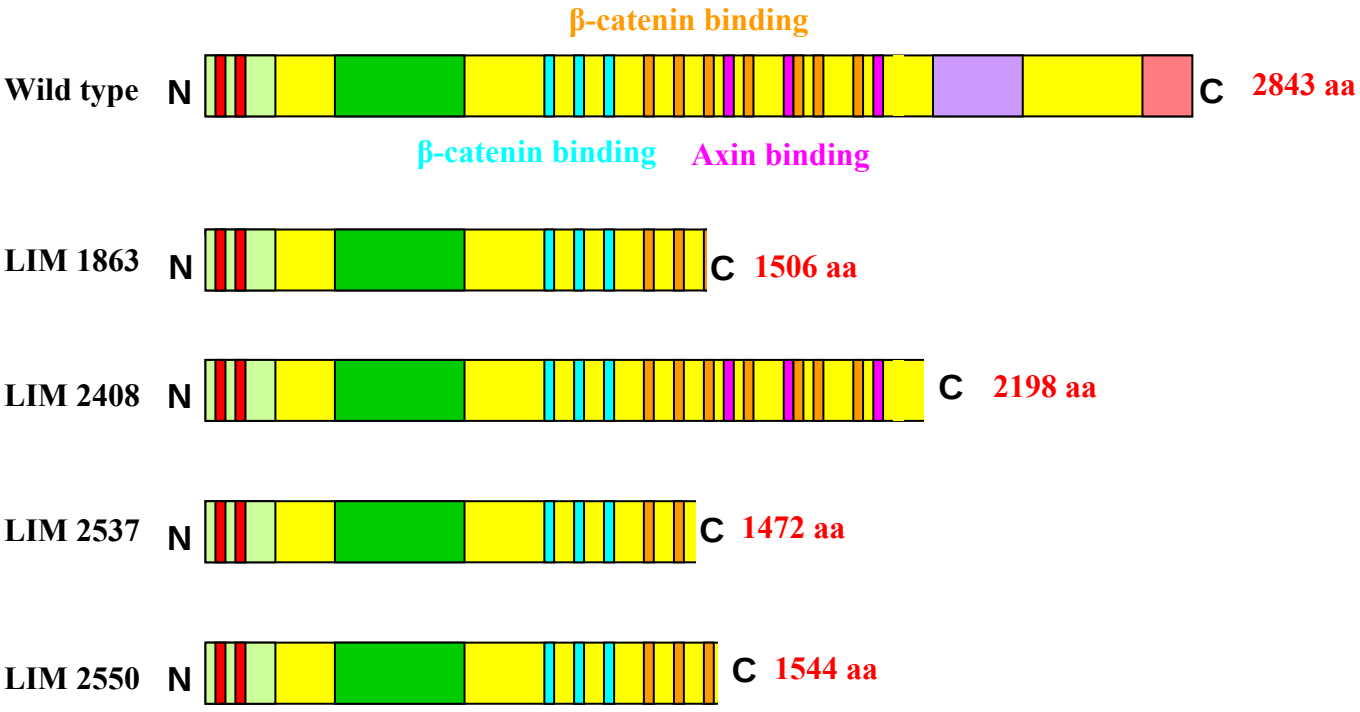

Figure 18. Schematic view of wt and the truncated APC proteins. The β-catenin binding sites are divided into three 15 amino acid repeats (blue) and seven 20 amino acid repeats (orange), while the Axin binding sites are depicted in pink. Numbers at right indicates the size of each protein. N, N-terminal; C, C-terminal.

The wild type APC proteins contain key elements that to some extent were retained in the different mutant proteins. The β-catenin binding sites can be divided into three 15 amino acid repeats (blue in Figure 18) and seven 20 amino acid repeats (orange in Figure 18). The 20 amino acid repeats bind β-catenin with a higher affinity than the 15 amino acid repeats and within the seven 20 amino acid repeats the third binding site exhibits the highest affinity for β-catenin. The three Axin binding sites (pink in Figure 18) are interspersed between the 20 amino acid repeats. Since the degradation of β-catenin is a key function of the APC protein, one would expect loss of the β-catenin binding sites to confer a greater selection advantage to tumour cells harbouring these mutations.

One can see that LIM 2408, which displayed a heterozygous mutation in APC, was the only cell line that retained both the β-catenin and Axin binding sites, thus allowing the formation of the β-catenin destruction complex in the Wnt signalling pathway and the subsequent degradation of β-catenin. Consequently it is likely that full transformation of these cells may have required mutations in another pathway, such as the ERK-MAPK pathway; and indeed homozygous mutation in B-Raf was confirmed (Table 14).

LIM 1863 retained only a few β-catenin binding sites, not including the third 20 amino acid repeat, and displayed a homozygous mutation (or LOH) in APC. Therefore the APC mutation may have been sufficient for the fully transformed phenotype, and indeed no additional mutations in the ERK-MAPK pathway were found (Table 14).

For LIM 2537, displaying a heterozygous mutation in APC, only a few binding sites for β-catenin, not including the 3rd, were retained and an additional mutation in B-Raf, a homozygous, was confirmed (Table 14).

LIM 2550 displayed a homozygous mutation (or LOH) in APC, and a heterozygous mutation in K-Ras was also found (Table 14), which could be due to the retention of the 3rd β-catenin binding site.

6.3 TGFβRII and BAX

According to several studies the most common microsatellite mutation in TGFβRII and BAX genes is a -1 frame-shift leading to a premature stop and resulting in a truncated protein. These observations were confirmed by the results obtained in this project (Table 13). The premature stop induced by the -1 frame-shift was found within the same exon as the frame-shift mutation for the BAX gene, but for the TGFβRII gene the stop codon was located in the following exon, exon 4, which was sequenced as well. Mutations were only found within the microsatellites and not in any other parts of the sequenced exons indicating that the genomic sequence for the -1 frame-shift induced peptides are not altered, an important knowledge when generating antibodies to these peptides.

Mutations in genes containing microsatellites, such as in TGFβRII and BAX, are found in MSI colon cancers due to their deficient MMR system, which normally correct errors that might occur during DNA replication. Table 13 summarizes the results of these mutations in the LIM cell lines and in accordance with the literature they all occur in MSI cell lines, except in the case of LIM 1899. This cell line has been characterized through immunohistochemistry as a MSS cell line although it clearly displays mutations in both

TGFβRII and BAX genes. It is therefore likely that LIM 1899 had been wrongly classified and should in fact be considered a MSI cell line.

Immunohistochemistry is a technique that can be used to determine whether or not the MMR genes, most often hMLH1 and hMSH2, are mutated. The non mutated MMR proteins are localized in the nucleus; subcellular localization is normally assessed through antigen-antibody binding, which can be visualized using for example fluorophores or enzymes tagged to the antibodies. In the case of LIM 1899, immunohistochemistry revealed the presence of nuclear MMR proteins, indicating that the MMR proteins were not mutated and leading to a diagnosis of MSS. An explanation for the discrepancy between the immunohistochemistry results and the sequencing data could be that the proteins were mutated in the active site impairing their function and not in the antigen-antibody binding site, which resulted in nuclear staining thus giving a false positive signal.

Both the results and the literature support the notion that there is no obvious correlation between the TGFβ/BAX pathways and the ERK-MAPK/Wnt pathways. The pathways have been shown to affect different cellular parameters; apoptosis/growth inhibition and growth promotion respectively. While both pathways are important for the cancer phenotype the relative contribution of each is not clear. Therefore, cells displaying mutations in more that one pathway (e.g. TGFβ and ERK-MAPK) constitute an ideal model for assessing the relative importance of oncogenes and tumour suppressor genes, for example by re-introducing the full length TGFβRII protein or blocking the K-Ras protein.

7. Conclusion

The genetic analysis of different tumour samples has provided an essential way of gaining insight in the development and progression of colorectal cancer. Genetic alterations in signal transduction pathways, such as the ERK-MAPK and Wnt signalling pathways, have shown to play a crucial part in the initiation and maintenance of colorectal cancer. Furthermore, genetic instability either at the chromosomal (CIN) or at the nucleotide (MSI) level creates a permissive environment for mutations to take place and accumulate. In addition, analysis of the different mutations in tumour samples will aid in assessing the contribution of each signal transduction pathway to the tumour phenotype by for example RNA interference.

Because of the multifunctional properties of the APC protein, mutations in this gene make an important contribution to the formation as well as the progression of colorectal cancers. It is therefore crucial to analyze and characterize the mutations and their involvement in the tumour development.

I have screened a panel of colon carcinoma cell lines generated at the Ludwig Institute for Cancer Research, Melbourne, Australia, and detected multiple mutations in oncogenes (K-Ras and B-Raf) and tumour suppressors (APC, TGFβRII and BAX). On the basis of the information provided in this work, it will be possible to correlate the tumour cell phenotype to specific mutations and to investigate the role of individual

mutations in cellular characteristics, such as proliferation, differentiation and metastatic potential.

Moreover, genetic analysis of genes, such as TGFβRII and BAX, containing mutations in microsatellites will allow the generation of antibodies specific for the frame-shift induced peptides, with potential as diagnostic tools or even therapeutic agents.

8. Acknowledgements

I would like to thank my supervisors Dr. Francesca Walker and Dr. Hui-Hua Zhang in the Epithelial Biochemistry laboratory at the Ludwig Institute for Cancer Research in Melbourne, Australia, for giving me the opportunity to conduct my degree project with them. Their valuable input throughout the project was greatly appreciated. I also want to express my gratitude to Dr. Zhang for her excellent supervision during my laboratory work. In addition, I would like to thank the people at the Ludwig Institute, Melbourne, for their support and friendship. Finally, a special thanks to Docent Carina Hellberg at the Ludwig Institute for Cancer Research in Uppsala for reviewing my report.

9. Bibliography

1. Vogelstein, B. et al. Genetic alterations during colorectal-tumor development. *N Engl J Med* **319**, 525-32 (1988).
2. Ilyas, M. & Tomlinson, I. P. Genetic pathways in colorectal cancer. *Histopathology* **28**, 389-99 (1996).
3. van Es, J. H., Giles, R. H. & Clevers, H. C. The many faces of the tumor suppressor gene APC. *Exp Cell Res* **264**, 126-34 (2001).
4. Fodde, R., Smits, R. & Clevers, H. APC, signal transduction and genetic instability in colorectal cancer. *Nat Rev Cancer* **1**, 55-67 (2001).
5. Bos, J. L. ras oncogenes in human cancer: a review. *Cancer Res* **49**, 4682-9 (1989).
6. Behrens, J. The role of the Wnt signalling pathway in colorectal tumorigenesis. *Biochem Soc Trans* **33**, 672-5 (2005).
7. Bertholon, J., Wang, Q., Galmarini, C. M. & Puisieux, A. Mutational targets in colorectal cancer cells with microsatellite instability. *Fam Cancer* **5**, 29-34 (2006).
8. Blanes, A. & Diaz-Cano, S. J. Complementary analysis of microsatellite tumor profile and mismatch repair defects in colorectal carcinomas. *World J Gastroenterol* **12**, 5932-40 (2006).
9. Bodmer, W. F. Cancer genetics: colorectal cancer as a model. *J Hum Genet* **51**, 391-6 (2006).
10. Fang, J. Y. & Richardson, B. C. The MAPK signalling pathways and colorectal cancer. *Lancet Oncol* **6**, 322-7 (2005).
11. Adjei, A. A. Blocking oncogenic Ras signaling for cancer therapy. *J Natl Cancer Inst* **93**, 1062-74 (2001).
12. Pollock, P. M. & Meltzer, P. S. Lucky draw in the gene raffle. *Nature* **417**, 906-7 (2002).
13. Akagi, K. et al. Characterization of a novel oncogenic K-ras mutation in colon cancer. *Biochem Biophys Res Commun* **352**, 728-32 (2007).
14. Oliveira, C. et al. Distinct patterns of KRAS mutations in colorectal carcinomas according to germline mismatch repair defects and hMLH1 methylation status. *Hum Mol Genet* **13**, 2303-11 (2004).
15. Nagasaka, T. et al. Colorectal cancer with mutation in BRAF, KRAS, and wild-type with respect to both oncogenes showing different patterns of DNA methylation. *J Clin Oncol* **22**, 4584-94 (2004).
16. Noda, H. et al. Frequent involvement of ras-signalling pathways in both polypoid-type and flat-type early-stage colorectal cancers. *J Exp Clin Cancer Res* **25**, 235-42 (2006).
17. Deng, G. et al. BRAF mutation is frequently present in sporadic colorectal cancer with methylated hMLH1, but not in hereditary nonpolyposis colorectal cancer. *Clin Cancer Res* **10**, 191-5 (2004).
18. Davies, H. et al. Mutations of the BRAF gene in human cancer. *Nature* **417**, 949-54 (2002).

19. Lustig, B. & Behrens, J. The Wnt signaling pathway and its role in tumor development. *J Cancer Res Clin Oncol* **129**, 199-221 (2003).
20. Behrens, J. & Lustig, B. The Wnt connection to tumorigenesis. *Int J Dev Biol* **48**, 477-87 (2004).
21. Shimizu, Y. et al. Frequent alterations in the Wnt signaling pathway in colorectal cancer with microsatellite instability. *Genes Chromosomes Cancer* **33**, 73-81 (2002).
22. Samowitz, W. S. et al. APC mutations and other genetic and epigenetic changes in colon cancer. *Mol Cancer Res* **5**, 165-70 (2007).
23. Schneikert, J. & Behrens, J. The canonical Wnt signalling pathway and its APC partner in colon cancer development. *Gut* **56**, 417-25 (2007).
24. Rubinfeld, B., Albert, I., Porfiri, E., Munemitsu, S. & Polakis, P. Loss of beta-catenin regulation by the APC tumor suppressor protein correlates with loss of structure due to common somatic mutations of the gene. *Cancer Res* **57**, 4624-30 (1997).
25. Jiricny, J. The multifaceted mismatch-repair system. *Nat Rev Mol Cell Biol* **7**, 335-46 (2006).
26. Schwitalle, Y., Linnebacher, M., Ripberger, E., Gebert, J. & von Knebel Doeberitz, M. Immunogenic peptides generated by frameshift mutations in DNA mismatch repair-deficient cancer cells. *Cancer Immun* **4**, 14 (2004).
27. Grady, W. M. & Markowitz, S. Genomic instability and colorectal cancer. *Curr Opin Gastroenterol* **16**, 62-67 (2000).
28. Saeterdal, I., Gjertsen, M. K., Straten, P., Eriksen, J. A. & Gaudernack, G. A TGF betaRII frameshift-mutation-derived CTL epitope recognised by HLA-A2-restricted CD8+ T cells. *Cancer Immunol Immunother* **50**, 469-76 (2001).
29. Rampino, N. et al. Somatic frameshift mutations in the BAX gene in colon cancers of the microsatellite mutator phenotype. *Science* **275**, 967-9 (1997).
30. Banerjea, A. et al. Colorectal cancers with microsatellite instability display mRNA expression signatures characteristic of increased immunogenicity. *Mol Cancer* **3**, 21 (2004).
31. Kleivi, K. et al. Genome signatures of colon carcinoma cell lines. *Cancer Genet Cytogenet* **155**, 119-31 (2004).
32. Luchtenborg, M. et al. Mutations in APC, CTNNB1 and K-ras genes and expression of hMLH1 in sporadic colorectal carcinomas from the Netherlands Cohort Study. *BMC Cancer* **5**, 160 (2005).
33. Devine, P. L. et al. Expression of MUC1 and MUC2 mucins by human tumor cell lines. *Tumour Biol* **13**, 268-77 (1992).
34. Foster, H. M., Tay, D. L. & Whitehead, R. H. Changes in the DNA ploidy patterns of human colorectal carcinomas, subsequent to culture or xenografting. *J Surg Oncol* **45**, 4-9 (1990).
35. Whitehead, R. H., Macrae, F. A., St John, D. J. & Ma, J. A colon cancer cell line (LIM1215) derived from a patient with inherited nonpolyposis colorectal cancer. *J Natl Cancer Inst* **74**, 759-65 (1985).
36. Whitehead, R. H., van Eeden, P. & Lukeis, R. E. A cell line (LIM 2463) derived from a tubulovillous adenoma of the rectum. *Int J Cancer* **48**, 693-6 (1991).

37. Whitehead, R. H., Zhang, H. H. & Hayward, I. P. Retention of tissue-specific phenotype in a panel of colon carcinoma cell lines: relationship to clinical correlates. *Immunol Cell Biol* **70 (Pt 4)**, 227-36 (1992).

Appendix: Media

TAE 50x, 5L
1210g Trizma Base
102.5g sodium acetate
73g EDTA disodium salt dihydrate
DDW up to total volume
adjust pH to 7.5 with HCl or NaOH

Tris 1M, 1L
121.1g Trizma Base,
DDW up to total volume
adjust pH to 7.5 with HCl or NaOH

TBS 10x, 5L
121.1g Trizma Base
438.3g sodium chloride
DDW up to total volume
adjust pH to 7.5 with HCl or NaOH

TTBS 10L
10xTBS 1L
Tween 20 10ml
DDW up to total volume
adjust pH to 7.5 with HCl or NaOH

SDS sample buffer 2x

DDW	3.8 ml
10% SDS	1.6 ml
0.5M Tris-HCI, pH 6.8	1.0 ml
Glycerol	0.8 ml
2-Mercaptoethanol	0.4 ml
0.5% Bromophenol blue	0.4 ml

Solubilization buffer
25 mM HEPES
150 mM NaCl
1% Triton X-100
1% Deoxycholate
5 mM EDTA
2xProtease inhibitor cocktail tablets